NeuroImage: Clinical 30 (2021) 102523

Contents lists available at ScienceDirect

NeuroImage: Clinical

journal homepage: www.elsevier.com/locate/ynicl

Multimodal MRI staging for tracking progression and clinical-imaging correlation in sporadic Creutzfeldt-Jakob disease

Simone Sacco [a,b], Matteo Paoletti [c], Adam M. Staffaroni [d], Huicong Kang [d,e], Julio Rojas [d], Gabe Marx [d], Sheng-yang Goh [d], Maria Luisa Mandelli [d], Isabel E. Allen [f], Joel H. Kramer [d], Stefano Bastianello [g,h], Roland G. Henry [a], Howie.J. Rosen [d], Eduardo Caverzasi [a,1,*], Michael D. Geschwind [d,1,*]

[a] UCSF Weill Institute for Neurosciences, Department of Neurology, University of California San Francisco (UCSF), San Francisco, CA, USA
[b] Institute of Radiology, Department of Clinical Surgical Diagnostic and Pediatric Sciences, University of Pavia, Pavia, Italy
[c] Advanced Imaging and Radiomics Center, Neuroradiology Department, IRCCS Mondino Foundation, Pavia, Italy
[d] UCSF Weill Institute for Neurosciences, Department of Neurology, Memory and Aging Center, University of California San Francisco (UCSF), San Francisco, CA, USA
[e] Tongji Hospital of Tongji Medical College of Huazhong University of Science and Technology, Wuhan, China
[f] Department of Epidemiology and Biostatistics, University of California San Francisco San Francisco (UCSF), San Francisco, CA, USA
[g] Department of Brain and Behavioral Sciences, University of Pavia, Pavia, Italy
[h] Neuroradiology Department, IRCCS Mondino Foundation, Pavia, Italy

ARTICLE INFO

Keywords:
Prion
Jakob-Creutzfeldt
CJD
JCD
DTI
Mean diffusivity
Atrophy

ABSTRACT

Diffusion imaging is very useful for the diagnosis of sporadic Creutzfeldt-Jakob disease, but it has limitations in tracking disease progression as mean diffusivity changes non-linearly across the disease course. We previously showed that mean diffusivity changes across the disease course follow a quasi J-shaped curve, characterized by decreased values in earlier phases and increasing values later in the disease course. Understanding how MRI metrics change over-time, as well as their correlations with clinical deficits are crucial steps in developing radiological biomarkers for trials. Specifically, as mean diffusivity does not change linearly and atrophy mainly occurs in later stages, neither alone is likely to be a sufficient biomarker throughout the disease course. We therefore developed a model combining mean diffusivity and Volume loss (MRI Disease-Staging) to take into account mean diffusivity's non-linearity. We then assessed the associations between clinical outcomes and mean diffusivity alone, Volume alone and finally MRI Disease-Staging.

In 37 sporadic Creutzfeldt-Jakob disease subjects and 30 age- and sex-matched healthy controls, high angular resolution diffusion and high-resolution T1 imaging was performed cross-sectionally to compute z-scores for mean diffusivity (MD) and Volume. Average MD and Volume were extracted from 41 GM volume of interest (VOI) per hemisphere, within the images registered to the Montreal Neurological Institute (MNI) space. Each subject's volume of interest was classified as either "involved" or "not involved" using a statistical threshold of ± 2 standard deviation (SD) for mean diffusivity changes and/or −2 SD for Volume. Volumes of interest were MRI Disease-Staged as: 0 = no abnormalities; 1 = decreased mean diffusivity only; 2 = decreased mean diffusivity and Volume; 3 = normal ("pseudo-normalized") mean diffusivity, reduced Volume; 4 = increased mean diffusivity, reduced Volume. We correlated Volume, MD and MRI Disease-Staging with several clinical outcomes (scales, score and symptoms) using 4 major regions of interest (Total, Cortical, Subcortical and Cerebellar gray matter) or smaller regions pre-specified based on known neuroanatomical correlates.

Volume and MD z-scores correlated inversely with each other in all four major ROIs (cortical, subcortical, cerebellar and total) highlighting that ROIs with lower Volumes had higher MD and vice-versa. Regarding correlations with symptoms and scores, higher MD correlated with worse Mini-Mental State Examination and

Abbreviations: **sCJD**, Sporadic Creutzfeldt-Jakob disease; **PrD**, prion disease; **PrP^{Sc}**, scrapie isoform of the prion protein; **DWI**, diffusion-weighted imaging; **GM**, grey matter; **MD**, mean diffusivity; **DTI**, Diffusion tensor imaging; **HC**, Healthy controls; **MMSE**, Mini-mental state examination; **VOI**, volume of interest; **ROI**, Region of interest.

* Corresponding authors.
E-mail addresses: saccosimone88@gmail.com (S. Sacco), Michael.Geschwind@ucsf.edu (M.D. Geschwind).
[1] Drs. Caverzasi and Geschwind are co-senior authors.

https://doi.org/10.1016/j.nicl.2020.102523
Received 25 May 2020; Received in revised form 2 November 2020; Accepted 1 December 2020
Available online 11 December 2020

Barthel scores in cortical and cerebellar gray matter, but subjects with cortical sensory deficits showed lower MD in the primary sensory cortex. Volume loss correlated with lower Mini-Mental State Examination, Barthel scores and pyramidal signs. Interestingly, for both Volume and MD, changes within the cerebellar ROI showed strong correlations with both MMSE and Barthel. Supporting using a combination of MD and Volume to track sCJD progression, MRI Disease-Staging showed correlations with more clinical outcomes than Volume or MD alone, specifically with Mini-Mental State Examination, Barthel score, pyramidal signs, higher cortical sensory deficits, as well as executive and visual-spatial deficits. Additionally, when subjects in the cohort were subdivided into tertiles based on their Barthel scores and their percentile of disease duration/course ("Time-Ratio"), subjects in the lowest (most impaired) Barthel tertile showed a much greater proportion of more advanced MRI Disease-Stages than the those in the highest tertile. Similarly, subjects in the last Time-Ratio tertile (last tertile of disease) showed a much greater proportion of more advanced MRI Disease-Stages than the earliest tertile. Therefore, in later disease stages, as measured by time or Barthel, there is overall more Volume loss and increasing MD.

A combined multiparametric quantitative MRI Disease-Staging is a useful tool to track sporadic Creutzfeldt-Jakob- disease progression radiologically.

1. Introduction

Sporadic Creutzfeldt-Jakob disease (sCJD) is the most common form of human prion disease (PrD) and classically presents as a rapidly progressive dementia with ataxia and myoclonus, usually leading to akinetic mutism and death within a year or less from onset, but there are several subtypes with slower progression. Other motor symptoms, as well as higher cortical dysfunction and behavioral disturbances are also common (Appleby et al., 2009; Brown et al., 1986; Parchi et al., 1999; Prusiner, 1998; Rabinovici et al., 2006).

Conventional MRI with diffusion-weighted imaging (DWI) has high diagnostic sensitivity and specificity for sCJD. The classical MRI finding of sCJD is cortical and/or subcortical grey matter (GM) restricted diffusion (reduced mean diffusivity MD)(Shiga et al., 2004; Vitali et al., 2011). Of the primary pathological features of prion disease, reduced diffusion seems to correlate strongest with vacuolization, and to a lesser extent with PrP^{Sc} (scrapie isoform of the prion protein) deposition (Geschwind et al., 2009; Haïk et al., 2002; Kretzschmar et al., 1996; Manners et al., 2009).

Reduced diffusion, however, is limited for tracking disease progression, as MD changes over time in sCJD are non-linear and even change direction (Caverzasi et al., 2014a). We previously showed with quantitative diffusion tensor imaging (DTI) that GM MD has a quasi J- or U-shaped (flattening of the top of the J) temporal trajectory with three possible phases relative to normal MD. In the 1st phase, MD decreases and is reduced relative to controls. In the 2nd phase, MD is still reduced but begins to increase back towards normal. This is followed by a 3rd phase in which the slope of increasing MD flattens (hence quasi J-shape), and MD is either normal or more often increased relative to controls (Caverzasi et al., 2014a). This temporal course might prevent use of GM MD alone as an imaging biomarker in treatment trials. Furthermore, GM MD varies even between brain areas in single subjects, likely due to regions being in different disease stages with varying underlying neuropathological or neurophysiological abnormalities (Grau-Rivera et al., 2017; Vitali et al., 2019).

Brain atrophy usually is not an obvious early radiological finding by standard visual assessment in sCJD (De Vita et al., 2017; Finkenstaedt et al., 1996) and seems to occur only in the intermediate/late stages of the disease, particularly in subjects with prolonged disease courses (Finkenstaedt et al., 1996; Galvez and Cartier, 1984; Uchino et al., 1991; Ukisu et al., 2005). Quantitative volume assessment methods such as voxel-based morphometry (VBM) or cortical thickness evaluation, however, are more sensitive for detecting atrophy in sCJD or other prion diseases (Alner et al., 2011; Cohen et al., 2009; De Vita et al., 2013, 2017; Grau-Rivera et al., 2017).

Understanding how MRI metrics change during the course of sCJD is important for establishing their relationship with clinical outcomes and identifying optimal imaging outcome measures, which might help with designing treatment trials and prognostication for patients. As MD does not change linearly, and atrophy that is appreciated by visual assessment only occurs later in the disease course, neither alone is likely to be a sufficient biomarker throughout the disease course.

In this study, we sought to systematically correlate in sCJD, a range of clinical scales, scores and symptoms with brain GM Volume alone, MD alone and a "MRI Disease-Staging" model that combined both GM Volume and MD changes. We hypothesized that combining MD and volumetric measures might improve the clinical-radiological correlation compared with using either parameter alone.

2. Material and methods

2.1. Subjects

The 37 subjects used in this study were serial patients evaluated at the UCSF Memory and Aging Center (MAC) from June 2008 to September 2015 for rapidly progressive dementia research, ultimately diagnosed with probable (n = 10) (Geschwind et al., 2007) and/or definite (n = 27) sCJD (Kretzschmar et al., 1996) and who had a sufficient quality research 3 T brain MRI (Siemens Trio Syngo, Erlangen, Germany) that included high angular resolution diffusion imaging (HARDI) (see Supplemental material regarding patient selection). Table 1 shows the demographics of the sCJD and healthy control cohorts. For the sCJD cohort, the mean age was 64 ± 8 years (median 65, range 46–82), 20 (54%) were males, 36 (97%) were right-handed and one was left-handed. Thirty healthy subjects matched for age and sex (mean age 64 ± 10, median 66, range 45–78, 50% female) who underwent the same MRI protocol on the same scanner were selected from the UCSF MAC database as healthy controls (HCs). As shown in Supplemental Tables 1A and 1B, codon 129 polymorphisms MV and VV were over-represented and MM under-represented, and regarding molecular classifications, MM1 was underrepresented and MM2, VV1/2, MV1 and MV1/2 were overrepresented in our cohort compared to a typical North American or European sCJD cohort (Collins et al., 2006; Parchi et al., 1999). Subjects or their caregivers provided informed consent to participate in this study, approved by the UCSF Committee on Human Research.

2.2. Clinical assessment.

Each subject had a detailed standardized comprehensive neurological examination and the Mini-Mental State Examination (MMSE)(Folstein et al., 1975). Of 37 subjects with sCJD, 30 had modified Barthel index of activities of daily living (ADLs; "Barthel")(Shah et al., 1989) and 28 had the neuropsychiatric inventory (NPI)(Cummings, 1997). Only 22 of 37 subjects were able to undergo at least part of a one-hour battery of neuropsychological testing (Geschwind et al., 2013). All scales, scores and the neurological examinations used for statistical analysis were recorded ± 3 days from MRI scan date. The sCJD cohort on average had moderate dementia and was mild to moderately functionally impaired (Table 1).

Table 1
Clinical features of sporadic Creutzfeldt-Jakob patients and controls.

	Controls n = 30	sCJD n = 37
Age at first evaluation, years, mean +/- SD (median, range)	64 +/- 10 (66, 45–78)	64 +/- 8 (65, 46–82)
Sex, female (%)	50	46
Right-handed (%)	100	97
Time-Ratio mean +/- SD (median, range)		0.64 +/- 0.25 (0.71, 0.11–1)
Total disease duration, months, mean +/- SD (median, range)		16.27 +/- 8.19 (17, 3–34)
MMSE score, mean +/- SD (median, range)	29.4 +/- 1 (30, 26–30)	16 +/- 8 (18, 0–27)
Barthel index, mean +/- SD (median, range)	N/D	63.7 +/- 37 (77.5, 0–100) (n = 30)
NPI, mean +/- SD (median, range)	N/D	24.8 +/- 17 (21, 0–61) (n = 28)
CSF t-tau (pg/mL) mean (median, range)[b]		3699.4 (4079, 248–15308) (n = 32)
CSF protein 14–3-3		n = 35
Positive (%)		40
Negative or inconclusive (%)		60
EEG		n = 33
Periodic epileptiform discharges (PED) (%)		9
Slowing without PEDs (%)		60
Normal (%)		31
Pathologically-confirmed cases (n; %)		27; 73%

Time-Ratio: (time from onset of symptoms to MRI scan/ total disease duration. MMSE = Mini-Mental State Examination; t-tau = total tau; CSF = cerebrospinal fluid; NPI = neuropsychiatric inventory frequency × severity product score (score range 0–144).
[b] Abnormal value > 1200 pg/mL.

2.2.1. Neurological examination

Components of the history and neurological examination (U.S. National Alzheimer's Disease Research Center standardized exam) were noted for presence or absence of a sign or symptom. Certain neurological systems were considered involved if a subject had the following symptoms/signs: pyramidal, ≥ two of four signs: weakness, hyperreflexia, spasticity, pathological reflexes (i.e., Hoffman's, up-going toes, Babinski, Chaddock's); extrapyramidal, ≥ two of five signs: cogwheel rigidity, hypomimia, reduction in amplitude of movements (finger taps, foot taps or open and close fist), global bradykinesia and non-rubral tremor (kinetic or postural); cerebellar, ≥ one of these three signs: dysdiadochokinesia, rubral tremor, dysmetria; and visual system, visual disturbances in this cohort were usually signs and symptoms such as blurred vision, difficulty seeing at dusk and but not visual field loss. Visual hallucinations, diplopia and eye fatigue were not considered as visual disturbances for the purposes of localization or correlation with MRI findings. Astereognosis and agraphesthesia were considered as higher cortical sensory dysfunction.

Regarding motor features in the 37 sCJD subjects, five (14%) had a pyramidal syndrome (all were bilateral), 14 (38%) had an extrapyramidal syndrome (2 unilateral left-body; 12 bilateral), and 19 (51%) a cerebellar syndrome (2 unilateral left-body; 17 bilateral). Eight (22%) subjects had higher cortical sensorial deficit (2 unilateral left-body; 6 bilateral) and 15 (41%) had visual disturbances.

2.2.2. Cognitive composites

Participants were given a comprehensive standardized one-hour neuropsychological battery used by our center which included assessment of memory, executive, language and visuospatial domains (Kramer et al., 2003). Cognitive composites were created for data reduction and reducing multiple comparisons. A threshold of tests was specified to allow for some missing data but require a requisite number of tests to improve comparability across individuals (See Supplemental material) (Kramer et al., 2003; Staffaroni et al., 2018a).

2.2.3. Neuropsychiatric inventory

The 12-item NPI was scored as the sum of frequency × severity scores for all 12 behaviors (Cummings, 1997). For our analyses we used both this score, referred to as "Total NPI," as well as three specified frequency × severity NPI categories scores (apathy, disinhibition and aberrant motor behavior) with known neuroanatomical atrophy correlation (Rosen et al., 2005).

2.3. MRI acquisition

Details of the MRI protocol are shown in Supplemental material, but included sagittal T1-weigthed 3D MPRAGE (voxel size 1x1x1 mm^3) and HARDI dataset (in-plane resolution = 2.2 mm^2; TR/TE = 8000/109 ms; 64 non-collinear diffusion sensitization directions at b = 2000 s/mm^2, 1 at b = 0; integrated parallel acquisition technique acceleration (IPAT) factor = 2).

2.4. Image processing and analysis

2.4.1. T1 Imaging processing

Before preprocessing, all T1-weighted images were visually inspected for quality control. T1-weighted images underwent bias field correction using N3 algorithm, and segmentation was performed using SPM12 (Wellcome Trust Center for Neuroimaging, London, UK; http://www.fil.ion.ucl.ac.uk/spm; RRID:SCR_007037) unified segmentation (Ashburner and Friston, 2005). A group template was generated from the within-subject average gray and white matter tissues by nonlinear and rigid-body registration template generation using Diffeomorphic Anatomical Registration using Exponentiated Lie algebra (DARTEL) (Ashburner and Friston, 2011). Native subjects' space gray and white matter were normalized, modulated, and smoothed in the group template using intersubject transformations. The applied smoothing used a Gaussian kernel with ~4 mm full-width chalf-maximum. For statistical purposes, linear and nonlinear transformations between DARTEL's space and International Consortium for Brain Mapping (Mazziotta et al., 1995) was applied. Each subject's average subject segmentations were carefully inspected to ensure no major segmentation or normalization errors.

2.4.2. Diffusion imaging processing

Initial image preprocessing was performed using the FMRIB Software Library (FSL; http://www.fmrib.ox.ac.uk/fsl/). FSL's brain extraction tool was used for skull stripping both for T1-weighted and diffusion dataset. Preprocessing of the DTI datasets was performed using FSL's diffusion toolbox. Eddy current distortions and motion artifacts were corrected by registering each diffusion-sensitized volume to the b0 volume with an affine transform. After tensor diagonalization, whole-brain maps of voxel wise quantitative GM metrics of MD were obtained. For each subject, the b0 volume of the DTI dataset was registered to T1-weighted image through dedicated boundary-based registration (Greve and Fischl, 2009). T1-weighted image was registered to the Montreal Neurological Institute (MNI) standard stereotactic atlas using FSL's linear and nonlinear registration tool. The MD map was warped to MNI space using the transform estimated for the registration of the T1-weighted image to MNI space.

2.4.3. MD and Volume involvement map.

Average MD and Volume were extracted from a total of 82 GM volumes of interest (VOI), within the images registered to the MNI space. Specifically, the Freesurfer segmentation output (aparc + aseg file) was used to obtain, for each hemisphere, 36 cortical GM VOIs (Desikan et al., 2006), 4 subcortical GM VOIs (thalamus, caudate, putamen, pallidus) and 1 cerebellar cortical GM VOIs (Fischl et al., 2002). White matter was not analyzed in this study. To decrease the potential effect of partial volume artifact, a threshold intensity, average intensity of cerebral spinal fluid (CSF) extracted in ventricles + 2 standard deviations (SD)

was used to exclude voxels that were likely to contain a mixture of CSF with GM from the VOI boundary. We considered caudate, putamen, globus pallidum and thalami as subcortical VOIs.

Age-corrected z-scores for MD and Volume were computed for sCJD subjects using HCs. Subsequently each VOI in each subject was classified in a binary manner as either involved or not involved for MD changes and for Volume loss using as statistical threshold of MD average +/- 2 SD from HCs for that VOI, and Volume average of −2 SD from HCs for that VOI.

2.4.4. Staging of the VOIs

We initially performed a voxel-based approach of MD maps to correlate with clinical scores and symptoms but could not find any correlations after multi-comparison correction (data not shown). We therefore then used a VOI approach. As MD changes are not only non-linear, but are J- or even U-shaped over time, and Volume loss tends to occur later in, the disease course (Caverzasi et al., 2014a, 2014b; Grau-Rivera et al., 2017), we developed an MRI Disease-Staging combining Volume and MD information, staging each single VOI for each subject as summarized in Table 2 and shown in Fig. 1. Our hypothesis was that a multi-parameter approach, would improve the clinical-radiological correlation compared with either parameter alone.

2.5. Statistical analysis

As there was a large range for subject total disease durations, we calculated a Time-Ratio scale (defined as the ratio between time from onset of symptoms to MRI scan divided by total disease duration), from 0 to 1 non-inclusive, to account for when an MRI was done during a subject's total disease course (Caverzasi et al., 2014a).

For most statistical analyses, composites of VOIs, referred to as regions of interest (ROIs; e.g. right parietal lobe, bilateral medial temporal lobe, total GM), were used by calculating the weighted-average for the MD z-score, Volume z-score or MRI Disease-Staging, with each individual VOI weighted based on its volume in MNI space. For assessing relationships of MMSE, Barthel, Time-Ratio and Total NPI with MRI quantitative metrics (MD and Volume) and MRI Disease-Stage, we used four general major ROIs (cortical, subcortical, cerebellar and total GM). We used pre-specified ROIs or single VOIs based on expected regions of neuroanatomical involvement to assess relationships of composite cognitive scores, three specific subcategories of NPI (apathy, disinhibition and aberrant motor behavior) and other specific neurological symptoms with MRI quantitative metrics and with MRI Disease-Stage.

Here we list the ROIs and VOIs used to assess these relationships. For cognitive composite scores: Executive-score with frontal lobes and all subcortical ROIs (Chow and Cummings, 2007; Cummings, 1995); Memory-score with bilateral medial temporal lobes (Mesulam, 2000); Language-score with the left lateral temporal lobe; and Visuospatial-score with the right parietal lobe (Mesulam, 2000). We used the lateral left temporal lobe as the ROI due to the specific nature of the tests including in the Language-score composite , which included: the Peabody Picture Vocabularly Test, a measure of semantic knowledge with correlates in the left temporal pole (Mesulam, 2016); the mini Boston Naming Test (15 item), a measure of confrontational naming, most commonly shows associations with the lateral temporal lobe in neuroimaging studies (Baldo et al., 2013); and lastly. Finally, we included semantic/category fluency, which also has a temporal anatomy (Baldo et al., 2006; Birn et al., 2010). Lexical fluency tasks were not included in our Language-score composite as they have a greater frontal lobe anatomy (including the IFG) and are often considered as an executive function measure (Staffaroni et al., 2018b). The single left-handed subject did not have language testing and thus was not included in the Language-score composite.

Neuroanatomical regions used for correlates for the three specific NPI subcategories were: aberrant motor behavior with a composite of two VOIs, caudal and rostral anterior cingulate; apathy with right superior frontal gyrus; and disinhibition with rostral anterior cingulate (Rosen et al., 2005).

For clinical syndromes the following neuroanatomical regions used for correlates were: visual disturbances with a composite of both occipital lobe VOIs, as signs and symptoms did not include lateralized features such as homonymous anopsias; lateralized cerebellar syndromes (i.e. limb ataxia or dysmetria) with the ipsilateral cerebellar hemisphere VOI; pyramidal syndrome with a composite of contralateral precentral gyrus and paracentral lobule VOIs (Fernandez-Torre et al., 2011); and extrapyramidal syndrome with a composite of contralateral subcortical VOIs (Fernandez-Torre et al., 2011). For assessing the relationship with higher cortical sensory loss (i.e., astereoagnosis or agraphesthesia), we used a single VOI of the post-central gyrus.

We used Pearson correlations for most of our primary analyses as well as the relationship between MD and Volume within the general major ROIs (cortical, subcortical, cerebellar and total GM). For assessing the relationship of MRI parameters with clinical symptoms expressed as categorical variables, we used a general linear model (ANOVA) for detecting differences in MD z-score alone, Volume z-score alone and MRI Disease-Stage between subgroups of subjects with and without specific symptoms (e.g., pyramidal, extrapyramidal), using the GM ROIs noted above.

To further assess if MRI Disease-Stage correlated with measures of disease severity, the following was done: for each subject, we calculated the proportion of VOIs at each specific MRI Disease-Stage (1, 2, 3 or 4) among all involved VOIs at any stage 1–4 (i.e., MRI Disease-Stage > 0). Then the cohort was divided according to disease severity into equal-sized tertiles according to the Barthel (100, <100 to > 55, ≤ 55) or the Time-Ratio (<0.47, ≥0.47 to < 0.8, ≥0.8). To further increase the power to detect differences, we combined stages 1 and 2 (less advanced stages) and stages 3 and 4 (more advanced stages). We then compared the proportions of VOIs involved at stages 1 or 2 and stages 3 or 4 in first vs last tertile using a two-sided *t*-test.

The total NPI was scored as the sum of frequency × severity scores for all 12 behaviors (Cummings, 1997). We then assessed correlations between this score and value of MD, Volume and MRI disease-stage within the 4 general major ROIs (cortical, subcortical, cerebellar and total GM).

Our analysis was corrected for multiple comparisons. Using the False Discovery Rate method for ranking p-values (Benjamini and Hochberg, 1995; Glickman et al., 2014), the q-value for significance of the results was q = 0.035 for all Pearson correlation data presented in Tables 3 and 4.

Table 2
MRI Disease-Staging per volume of interest (VOI)[a] based on gray matter mean diffusivity (MD) and Volume.

MRI Disease-Stage	MD	Volume
0	Normal	Normal
1	Decreased	Normal
2	Decreased	Decreased
3	Normal due to "pseudo-normalization"	Decreased
4	Increased	Decreased

[a] Per aparc + aseg file output of the Freesurfer pipeline (Desikan et al, 2006; Fischl et al, 2002). In each volume of interest (VOI) MD is considered decreased if < 2 SD, or increased if > 2 SD, from healthy controls (HCs). Volume of a VOI is considered decreased if < 2 SD from HCs. See Methods for more details.

3. Results

3.1. Correlation among clinical scales or scores.

The Time-Ratio showed a strong negative correlation with Barthel (R −0.66, p = 0.0004) and a trend toward negative correlation with the MMSE (R −0.29, p = 0.08), suggesting that subjects later in their disease course showed worse impairment. Time-Ratio, however, had no

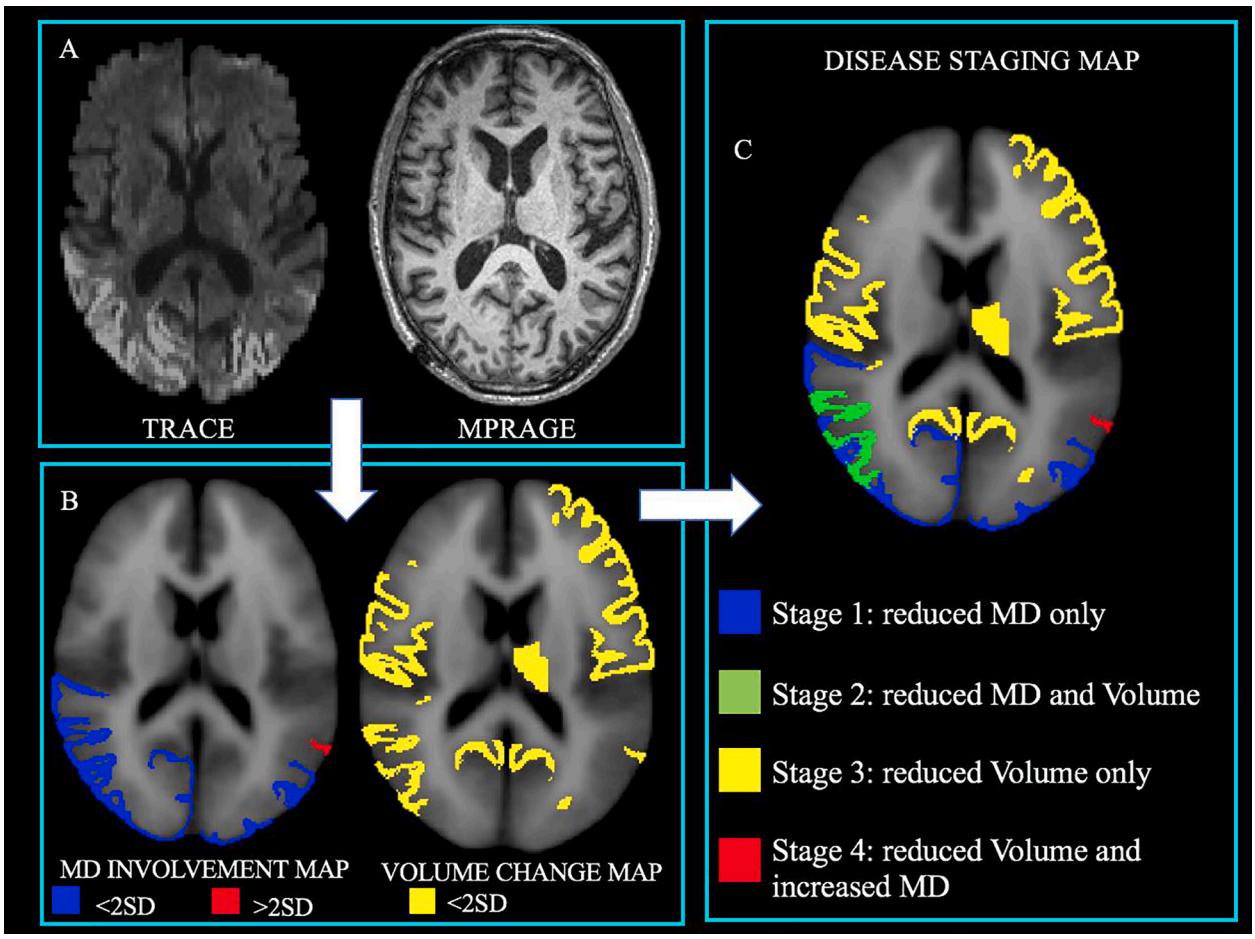

Fig. 1. MRI Disease-Staging process in each volume of interest (VOI) using mean diffusivity (MD) and Volume loss. (A) Left figure is an axial B2000 Trace DWI brain image and right is a T1MPRAGE of a single subject. (B) Mapping of MD (left figure) and Volume loss (right figure) of the subject compared to HCs onto MNI space. (C) MRI Disease-staging map: each VOI is assigned to a disease stage based on the MD being reduced, increased or no difference compared to HCs and Volume being reduced or not reduced compared to HCs. MRI Disease-Stages for each VOI are then used for correlation with clinical outcomes.

Table 3
Correlations between Volume and Mean Diffusivity z-scores.[a]

Gray Matter Region of interest (ROI)	Total	Cortical	Subcortical	Cerebellum
Pearson correlation coefficient (R); P-value (CI)	−0.54; 0.0005 (−0.74;−0.26)	−0.43; 0.009 (−0.66;−0.13)	−0.36; 0.029 (−0.61;−0.04)	−0.46; 0.004 (−0.73;−0.05)

[a] This able shows Pearson correlation coefficients between MD z-score and Volume z-score in total, cortical, subcortical and cerebellum ROIs. 95% confidence intervals (CI) are reported. Using the False Discovery Rate method for ranking p-values, the q-value for significance of the results was q = 0.035 correction)

correlation with Memory-score (R 0.32, p = 0.14), Executive-score (R 0.003, p = 0.98), Language-score (R − 0.007, p = 0.76), or Visuospatial-score (R −0.20, p = 0.36). The Barthel correlated strongly with the MMSE (R 0.68, p = 0.00003) and correlated with Memory-score (R 0.51, p = 0.03), but only trended toward positive correlation with Visuospatial-score (R 0.45, p = 0.07) and had no correlation with the Executive-score (R 0.22, p = 0.37) or Language-score (R 0.29, p = 0.24). We hypothesized that the cognitive composite scores overall did not correlate well with Time-Ratio or Barthel because the subgroup of patients who were able to perform the cognitive test battery used to derive the composite scores were earlier in the disease course or less functionally impaired, and thus the cognitive composites were not captured across the entire disease spectrum. Ad hoc analysis confirmed that those who could do the cognitive test battery (n = 22) were less functionally impaired (on Barthel) and trended towards being earlier in the disease course compared to the subgroup who could not (n = 15) do the cognitive battery (see Supplemental Material Section 2.1). Other correlations among scales and scores are shown in Supplemental material.

3.2. Correlation between Volume and MD z-scores at the ROI level.

Volume and MD z-scores correlated inversely with each other in all four major ROIs (cortical, subcortical, cerebellar and total) (Table 3). Thus, ROIs with lower Volumes had higher MD and vice-versa, consistent with our prior 1.5 T data (Caverzasi et al., 2014a) and our MRI Disease-Stage model.

3.3. Correlations of MD z-score with clinical outcomes (scales, scores and symptoms).

Various clinical outcomes correlated with MD z-scores, but with differences in directionality. Regarding those correlating with higher MD, in general, more cognitively and functionally impaired subjects (lower MMSE and Barthel) had higher MD values (Table 4). Specifically, lower Barthel scores correlated with higher total and cerebellar MD, but not with cortical or subcortical MD. The relationship between MD z-score and Barthel are shown in Fig. 2A.

Table 4
Relationship between quantitative MRI metrics and clinical outcomes.

Pearson correlations (R)[a] between quantitative MRI metrics in major Regions of Interest (ROIs)ˆ and clinical scales			
Clinical scales/ Gray Matter ROIs	MD z-score	Volume z-score	MRI Disease-Staging
	R; P value (CI)	R; P value (CI)	R; P value (CI)
Barthel (n = 30)			
Total	**−0.42; 0.025 (−0.68, −0.07)**	0.36; 0.045(0.01, 0.64)	**−0.44; 0.013 (−0.69, −0.102)**
Cortical	−0.37; 0.045 (−0.65, −0.02)	0.27; 0.15	−0.32; 0.08 (−0.61, 0.04)
Subcortical	0.25; 0.17	**0.41; 0.021 (0.07, 0.68)**	−0.32; 0.08 (−0.61, 0.04)
Cerebellar	**−0.49; 0.006 (−0.72, −0.153)**	**0.53; 0.002 (0.20, 0.746)**	**−0.57; 0.001 (−0.77, −0.262)**
MMSE (n = 37)			
Total	0.07; 0.67	**0.37; 0.022 (0.06, 0.62)**	**−0.52; 0.0009 (−0.72, −0.23)**
Cortical	0.19; 0.25	**0.34; 0.034 (0.03, 0.65)**	**−0.48; 0.002 (−0.67, −0.19)**
Subcortical	−0.11; 0.48	**0.40; 0.014 (0.09, 0.64)**	**−0.54; 0.0005 (−0.73, −0.26)**
Cerebellar	**−0.44; 0.006 (−0.67, −0.14)**	**0.37; 0.024 (0.05, 0.62)**	**−0.45; 0.006 (−0.67, −0.14)**
Time-Ratio (n = 37)			
Total	0.32; 0.06 (−0.004, 0.58)	−0.17; 0.3	0.23; 0.16
Cortical	0.0.28; 0.08 (−0.05, 0.55)	−0.13; 0.4	0.17; 0.31
Subcortical	−0.04; 0.8	−0.17; 0.3	0.07; 0.6
Cerebellar	**0.36; 0.03(0.04, 0.62)**	−0.26; 0.11	0.34; 0.04(0.01, 0.6)
Total NPI (n = 28)			
Total	0.03;0.86 (−0.35;0.4)	−0.07;0.7 (−0.43;0.31)	0.13;0.48 (−0.26;0.48)
Cortical	0.04;0.84 (−0.34;0.44)	−0.02;0.9 (−0.39;0.35)	0.14;0.47 (−0.25;0.49)
Subcortical	**−0.62;0.0005 (−0.8;−0.32)**	−0.15;0.34 (−0.5;0.24)	0.18;0.36 (−0.21;0.52)
Cerebellar	0.21;0.26 (−0.18;0.54)	−0.17;0.38 (−0.51;0.22)	0.07;0.7 (−0.31;0.43)
Pearson correlations between quantitative MRI metrics in pre-determined ROIsˆ and neurocognitive composed score assessing specific functions			
Composite neurocognitive score/ Gray Matter ROIs	MD z-score	Volume z-score	MRI Disease-Staging
	R; P value (CI)	R; P value (CI)	R; P value (CI)
Visuospatial-score (n = 22)			
Right Parietal lobe	0.26; 0.22	0.12; 0.58	**−0.60; 0.002 (−0.81, −0.24)**
Memory-score (n = 22)			
Bilateral medial temporal lobe	−0.05; 0.82	0.29; 0.18	−0.34; 0.11
Executive Function-score (Executive-score) (n = 22)			
Subcortical	0.06; 0.77	0.14; 0.51	**−0.58; 0056 (−0.8, −0.21)**
Bilateral frontal lobe	0.30; 0.17	0.04; 0.84	0.33; 0.14
Language-score (n = 22)			
Left lateral temporal lobe	0.19; 0.38	0.23; 0.30	−0.26; 0.25
Pearson correlations between quantitative MRI metrics in pre-determined ROIsˆ and specific Neuropsychiatric Inventory categories			
NPI category/ Gray Matter ROIs	MD z-score	Volume z-score	MRI Disease-Staging
	R; P value(CI)	R; P value(CI)	R; P value(CI)
Apathy (n = 28)			
Right superior frontal gyrus	0.22;0.25 (−0.17;0.55)	−0.15;0.43 (−0.5;0.24)	0.08;0.66 (−0.3;0.44)
Disinhibition (n = 28)			
Rostral anterior cingulate	−0.15;0.43 (−0.5;0.24)	−0.26;0.18 (0.58;0.13)	0.27;0.16 (−0.11;0.58)
Aberrant motor behavior (n = 28)			
Caudal and rostral anterior cingulate	**−0.44;0.01 (−0.7;−0.08)**	0.04;0.84 (−0.34;0.41)	−0.13;0.48 (−0.48;0.26)
Comparison (ANOVA) of MRI quantitative metrics in pre-determined ROIs between subjects with and without specific symptoms			
Clinical findings/ Gray Matter ROIs	MD z-score	Volume z-score	MRI Disease-Staging
Pyramidal syndrome (n = 37)			
Contralateral precentral gyrus and paracentral lobule	No differences (P value > 0.1)	Lower Volume in symptomatic patients (p value = 0.002)	More ad advanced MRI Disease-Stages in symptomatic patients (p value = 0.002)
Extrapyramidal syndrome (n = 37)			
Contralateral putamen, caudate, pallidum and thalamus	No differences (P value > 0.1)	No differences (P value > 0.1)	No differences (P value > 0.1)
Cortical sensory deficit (Left astereognosis and agraphesthesia) (n = 37)			
Right post-central gyrus	Lower MD in symptomatic patients (p value = 0.02)	No differences (P value > 0.1)	More advanced MRI Disease-Stages in symptomatic patients (p value = 0.007)
Cortical sensory deficit (Right astereognosis and agraphesthesia) (n = 37)			
Left post-central gyrus	No differences (P value > 0.1)	No differences (P value > 0.1)	No differences (P value > 0.1)
Cerebellar syndrome (n = 37)			
Ipsilateral Cerebellum	No differences (P value > 0.1)	No differences (P value > 0.1)	No differences (P value > 0.1)
Visual deficits (n = 37)			
Occipital lobe	No differences (P value > 0.1)	No differences (P value > 0.1)	No differences (P value > 0.1)

Summary description of Table results**:**

- **MD** correlates negatively with Barthel and MMSE, indicating worse scores are associated with higher MD values and vice-versa. MD correlates positively with Time-Ratio (defined as the ratio between time from symptoms onset to MRI scan divided by total disease duration), indicating that subjects with higher Time-Ratio (later in their disease course at the time of MRI scan) show higher MD values and vice-versa.
- **Volume** correlates positively with Barthel and MMSE, indicating worse scores are associated with lower Volume and vice-versa.
- **MRI disease-staging** correlates negatively with Barthel, MMSE, Executive and Visuospatial scores indicating worse scores to be associated with more advanced MRI disease-stages and vice-versa. MRI disease-staging correlates positively with Time-Ratio, indicating that subjects with higher Time-Ratio (later in their disease course at time of MRI scan) show more advanced MRI disease-stages vice-versa.

[a] **Bold** results indicate statistically significant correlations at $p < 0.035$. (Using the False Discovery Rate method for ranking p-values, the q-value for significance of the results was $q = 0.035$ correction). Underlined results indicate trends toward correlation at $0.1 < p < 0.35$. 95% confidence intervals (CI) are reported only for statistically significant correlations and trends toward correlation. ˆSee text for a detailed description of ROIs

Lower MMSE scores correlated with higher cerebellar MD but no other ROIs. Time-Ratio showed a positive correlation with MD z-score only in cerebellum but trended toward positive correlation with total GM MD and cortical MD, suggesting that subjects later in their disease course have higher MD values, particularly in the cerebellum.

Higher cortical function deficits were associated with lower MD. Specifically, subjects with left body astereognosis and/or agraphesthesia had lower MD in the right postcentral gyrus. Subjects with worse overall psychiatric symptoms (higher Total NPI) had lower subcortical MD. The

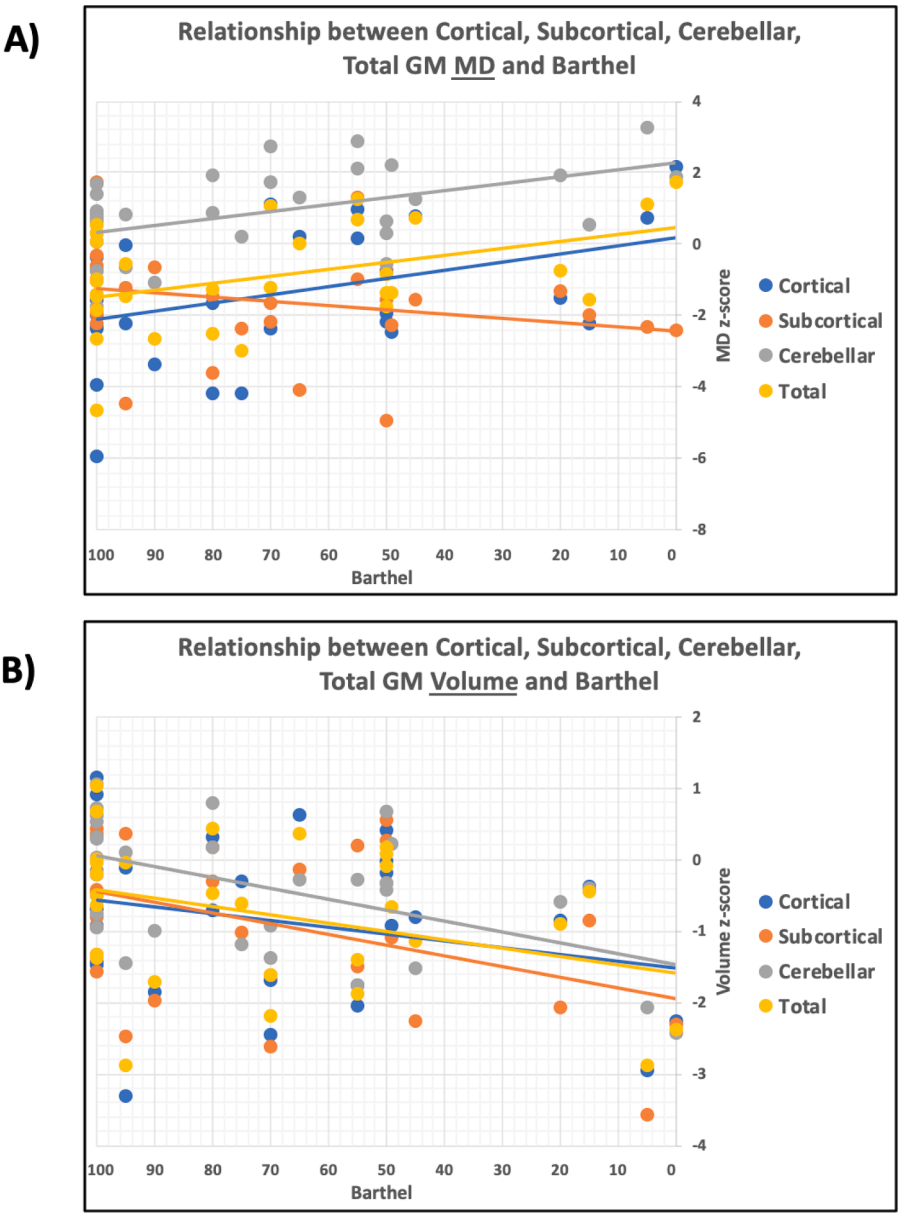

Fig. 2. Relationship between Barthel and MRI gray matter MD or Volume. Relationship between Barthel and MRI gray matter MD and Volume. These graphs show the relationship between Barthel scores (X axis) and (A) MD z-score (Y axis) or (B) Volume z-score within Cortical, Subcortical, Cerebellar, and Total gray matter (GM) ROIs. Note the Barthel is plotted on the X-axis going left to right from higher (more functional) to lower scores (less functional). Subjects with lower Barthel scores (more impaired) show higher MD z-scores in all ROIs except for the Subcortical GM. For Subcortical GM, the relationship is in the opposite direction, with more impaired subjects having lower MD, and conversely less impaired subjects having higher MD in the striatum and thalamus. In (B) relationship between Barthel scores and Volume z-score suggests that subjects with lower Barthel scores (more impaired) have lower Volume z-score in all major ROIs.

total NPI did not, however, correlate with total GM, cortical, or cerebellar MD. Among the three specific categories of the NPI (apathy, disinhibition and aberrant motor behavior) with prior defined neuroanatomical correlation (Rosen et al., 2005), the only correlation was negative, between MD in the anterior cingulate ROI and aberrant motor behavior, meaning lower MD values were associated with worse (higher) NPI category scores (Table 4). No other relationships were found with composite cognitive scores or major symptom categories

3.4. Correlation of Volume z-score with clinical outcomes (scales, scores and symptoms)

We next explored correlations with Volume. MMSE correlated positively in all major ROIs, whereas Barthel correlated positively in cerebellar and subcortical ROIs (Table 4), suggesting that more cognitively and functionally impaired subjects have greater atrophy. The relationship between Volume z-score and Barthel is shown graphically in Fig. 2B. Interestingly, Time-Ratio did not correlate with any major ROI. Subjects with a pyramidal syndrome, however, had less Volume in the contralateral precentral gyrus and paracentral lobule than those without this syndrome. No other correlations or relationships were identified with composite cognitive scores or other symptom categories.

3.5. Correlation of MRI Disease-Staging with clinical outcomes (scales, scores and symptoms)

Overall, compared with either Volume or MD z-score alone, MRI Disease-Staging showed correlations (mostly negative) with more clinical outcomes and with slightly higher correlation coefficients in most ROIs, although CIs overlapped (Table 4). Specifically, MMSE correlated negatively (lower MMSE, higher MRI Disease-Staging score) in all four major ROIs. Barthel also correlated negatively in total and cerebellar ROIs and trended negatively in subcortical and cortical ROIs. After multiple comparison correction, Time-Ratio did not correlate with any ROIs, however, the p-value for the correlation of Time-Ratio and MRI Disease-stage within the cerebellum was very close to the statistical significance ($p = 0.037$ with 0.035 of cut off after multiple comparison correction). This suggests that subjects temporally later in their disease course may have more advanced MRI Disease-Stages in the cerebellum (lower Volume and higher MD). To assess if the 51% of our cohort whom

had cerebellar signs had cerebellar MRI differences, we compared MRI findings (MD, Volume, MRI Disease-Staging) in cerebellar ROIs between sCJD patients with or without a cerebellar syndrome. We found no statistical difference in MD, Volume or MRI disease Stage values, however (Table 4).

Regarding cognitive assessments, Executive-score correlated, negatively, with only subcortical ROIs but not with frontal lobes. Visuospatial-score correlated, negatively, with the right parietal lobe ROI. Thus, subjects with worse Executive and Visuospatial scores had higher MRI Disease-Stage (increased MD, reduced Volume) in these respective regions than those with better scores. Neither Language-score nor Memory-Score correlated with MRI Disease-Stage (Table 4).

Subjects with pyramidal symptoms and left body astereognosis and/or agraphesthesia had higher MRI Disease-Stages (increased MD, reduced Volume) in the contralateral precentral and paracentral gyrus and right postcentral gyrus, respectively, than subjects without these features (Table 4).

3.6. Number and sum of VOIs involved at each MRI Disease-Stage.

Regarding the number of VOIs involved by MD and/or Volume (i.e., MRI Disease Stage 1–4), on average only 32 ± 20 out of 80 total VOIs (40%; median 30, range 4–78) were involved per subject. The most commonly involved VOI was the right lateral occipital cortex (n = 27; 73%); the least involved was the left hippocampus (n = 3; 8%; see Supplemental Table 2). For each VOI, the mean number of subjects with involvement was 16 ± 6 out of 37 (43%; median 15, range 3–27). The average percent of brain Volume involved at each MRI Disease-Stage for the cohort is shown in Fig. 3. Note that on average 60% of the brain was MRI Disease-Stage 0, not involved in terms of MD or Volume. Among the 40% of VOIs involved, 60% were Stage 1, with only reduced MD.

3.7. Relationship between number of VOIs involved by MRI Disease-Stage 1–4 and either the Barthel or Time-Ratio

There was no correlation between the Barthel or the Time-Ratio and either the percent of VOIs or percent of Volume of VOIs involved (not shown). We then limited this analysis to only correlate with involved regions by considering only VOIs with MRI Disease-Stages 1–4. Examining the percent of VOIs involved at each MRI Disease-Stage, only MRI Disease-Stage 4 (increased MD, reduced Volume) correlated, positively, with Time-Ratio (R 0.33, p = 0.04) and, negatively, with Barthel (R −0.38, p = 0.006). Examining the percent of Volume involved at each MRI Disease-Stage, both MRI Disease-Stage 3 (normal MD, reduced Volume) and Stage 4 correlated, negatively, with Barthel (R −0.42, p = 0.02; R −0.40, p = 0.03, respectively), whereas MRI Disease-Stage 4, correlated, positively, with Time-Ratio (R 0.37, p = 0.02). These data suggest that subjects with more advanced disease have reduced Volume and either normal or increased MD in more VOIs than less advanced (by Barthel or Time-Ratio) subjects.

3.8. Relationship of MRI Disease-Staging with disease severity scales (Barthel and Time-Ratio) by tertiles

Next, in order to increase power to detect relationships, rather than examining correlations along an entire scale spectrum, we looked at the distributions of MRI Disease-stages among subjects subdivided in groups according to two measures of disease severity, Barthel and Time-Ratio. Given that for each VOI, more than half of subjects did not show involvement (MRI Disease-Stage 0), for this analysis we only considered involved VOIs (MRI Disease-Stage 1–4) to avoid giving too much weight to the MRI Disease-Stage 0, uninvolved brain regions.

Subjects in the cohort with Barthel scores (n = 30) and with Time-Ratio (n = 37) were subdivided into tertiles. The distribution of the MRI Disease-Stages within the regions involved (MRI Disease-Stage > 0) in each tertile group is shown in Fig. 4. There was no difference in the

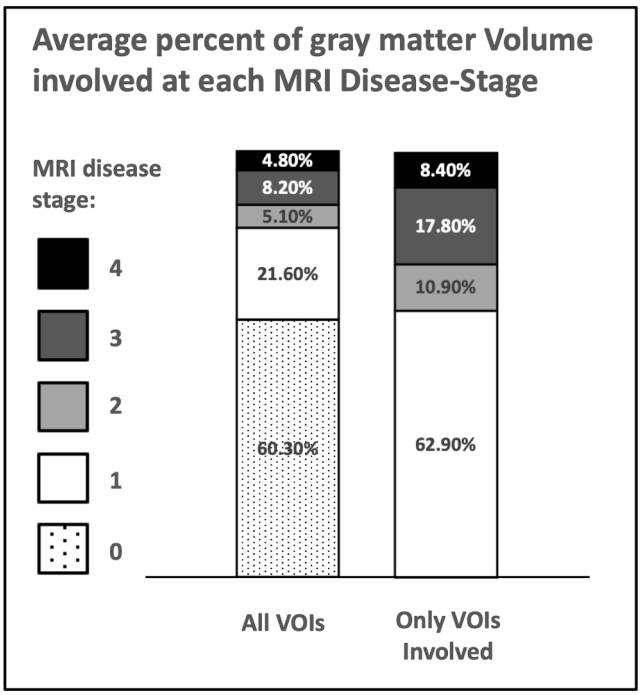

Fig. 3. Average percent of gray matter Volume involved at each MRI Disease-Stage Average percent of gray matter Volume involved at each MRI Disease-Stage. The average percent of volumes of interest involved at each MRI Disease-Stage in the cohort considering all volumes of interest (VOIs) regardless of whether they were involved or not (i.e. includes volume not involved; left bar graph) or considering only involved VOIs (i.e. MRI Disease-Stage 1–4; right bar graph). For all subjects, the average MRI Disease-Stage was calculated for each VOI and then multiplied by the volume of each VOI to calculate these values. VOIs MRI Disease-Stages as follows: 0 = no abnormalities; 1 = decreased mean diffusivity only; 2 = decreased mean diffusivity and Volume; 3 = normal ("pseudo-normalized") mean diffusivity, reduced Volume; 4 = increased mean diffusivity, reduced Volume. A similar analysis examining not percent of total volume, but percent of VOIs (not corrected for size of VOI) involved showed nearly identical results (not shown).

distribution of MRI Disease-Stages 1–4 among the Barthel or the Time-Ratio tertiles. Therefore, to better detect differences, we combined certain stages. As a key aspect of our model is mean diffusivity, which is an almost pathognomonic diagnostic imaging feature of this disease, we focused on the state of MD. We therefore combined stages 1 and 2 (both of which have restricted MD; less advanced stages) and stages 3 and 4 (which both have increased or pseudo-normalization of MD; more advanced stages). Subjects in the lowest Barthel tertile showed a much greater proportion of more advanced MRI Disease-Stages than the highest tertile (two-sided *t*-test, p = 0.03), and similarly, subjects in the last Time-Ratio tertile showed a much greater proportion of more advanced MRI Disease-Stages than the earliest tertile (two-sided *t*-test, p = 0.02). This, generally supports findings in our prior analysis in Section 3.7, showing that subjects whose disease was more progressed had more brain regions (VOIs) with higher MRI Disease-Stages (increased MD, reduced Volume).

As shown in Section 3.5 (Correlation of MRI Disease-Staging with clinical outcomes), whereas Barthel had correlations with MRI Disease-Stage in many ROIs, Time-Ratio correlated with MRI Disease-Stage only in cerebellar GM. To further explore possible relationships of Time-Ratio with MRI Disease-Stage, we compared the mean MRI Disease-Stage within each involved VOI (Stages 1–4) and major ROI for subjects in the earliest versus the latest Time-Ratio tertiles. This analysis, not assessed for statistical significance because of multiple comparisons, shows that subjects in the latest Time-Ratio tertile had more advanced MRI Disease-Stages in almost all VOIs than did those in the earliest Time-

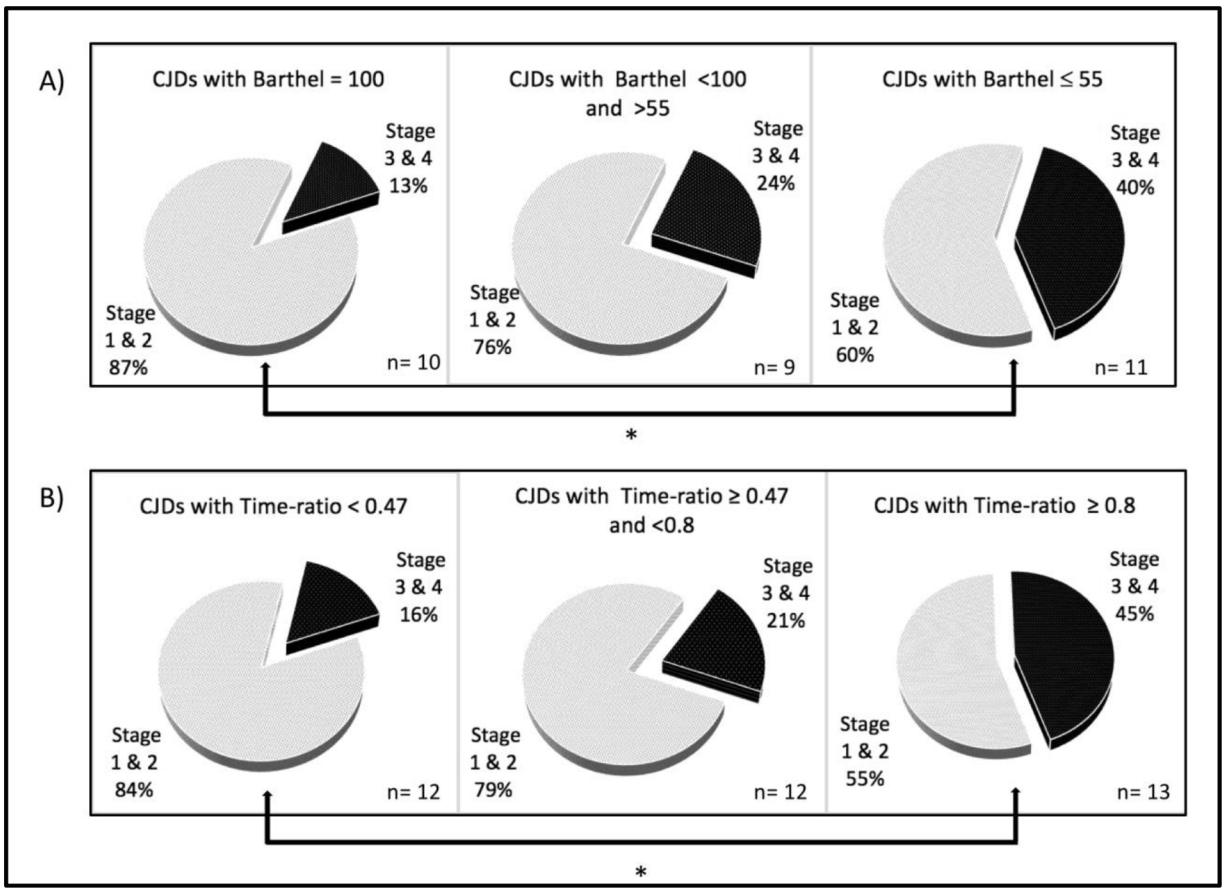

Fig. 4. Relationship between Disease-Stage and Barthel or Time-Ratio Tertiles. Subjects in the cohort with available Barthel scores (A; n = 30) and with Time-Ratio (B; n = 37) were subdivided into tertiles based on these scores (see Results). A) Patients with highest Barthel tertile (Barthel = 100) had a statistically significant difference (*; $p < 0.03$, two-sided *t*-test) in the percent of VOIs involved at disease stages 1–2 versus 3–4 compared to patients with lowest Barthel tertile (Barthel ≤ 55). B) Patients in the earliest Time-Ratio (lower than 0.47; i.e. closer to onset) showed a statistically significant difference (* $p < 0.02$, two-sided *t*-test) in the percent of VOIs involved at MRI disease stages 1–2 versus 3–4 compared to patients in the latest Time-Ratio tertile (≥0.8; i.e., closer to the end of disease-course). As this Figure suggests, there appears to be a direct relationship between the MRI Disease-Staging and the Barthel as well as Time-Ratio. Thus, in later disease stages, as measured by Time-Ratio or Barthel, there is a larger percent of VOIs with reduced Volume and increasing MD.

Ratio tertile (Supplemental Table 3). This suggests that, in general when a region is involved (reduced Volume and/or abnormal MD), in subjects who are later in their disease course that region is more likely to be at a more advanced MRI Disease-Stage and the converse. Thus, MRI Disease-Stage tracks disease course in both early and late disease stages, and therefore in most of the VOIs that are involved (reduced Volume and/or abnormal MD) there is a progression toward higher MD and reduced Volume (i.e. atrophy or Volume loss) at later disease stages.

4. Discussion

This study systematically evaluated the correlation of clinical outcomes (clinical scales, scores and symptoms) with two important MRI features of sCJD, MD abnormalities and Volume loss. As our and others' previous research had shown that radiological parameters might change variably in different stages of PrD (Caverzasi et al., 2014a, 2014b; Grau-Rivera et al., 2017), we developed a novel MRI Disease-Staging scale with four serial stages that can be applied to each VOI: 1. Reduced MD and normal Volume early in the disease process; 2. Reduced MD and initial Volume loss; 3. Volume loss associated with normal MD; and 4. Further Volume loss associated with increased MD. Thus, in brain regions with early involvement, there is primarily decreased MD with no or minimal Volume loss. As disease in a brain region advances, progressive Volume loss (atrophy) is associated with higher MD values (Caverzasi et al., 2014a, 2014b; Grau-Rivera et al., 2017). As we hypothesized, a quantitative multi-parameter approach combining MD and Volume changes shows correlations with more clinical outcomes than either MD or Volume alone.

There are at least two main reasons why our MRI Disease-Staging appears to work better for clinical-imaging correlation than MD changes alone: 1. MD change over-time in sCJD is non-linear (Caverzasi et al., 2014a), and 2. MD increases during a disease stage when atrophy occurs (discussed later). Regarding the first reason, an individual with sCJD can simultaneously have some regions with increased MD, some with decreased MD, and some with normal MD (Grau-Rivera et al., 2017). This is because as a brain region becomes affected, initially there is a phase of decreased MD, but if the disease progresses for sufficient time, that region will eventually a stage of increasing MD (Caverzasi et al., 2014a). Therefore, for any brain region, clinical outcomes would not correlate with MD alone (which changes non-linearly) throughout the entire course of the disease (decreased, then increased MD), but for our current study we predicted they might correlate with either the increasing or the decreasing phase alone of MD change. In line with this hypothesis, we found that certain clinical outcomes correlated with higher MD and others with lower MD. Patients with more global impairment (based on Barthel or MMSE) showed higher cortical and cerebellar MD values, whereas patients with more neuropsychiatric symptoms (higher NPI) and higher cortical sensory dysfunction showed lower MD values within the subcortical GM and the postcentral gyrus, respectively. We postulate that the latter may be because identifying

deficits such as agraphesthesia and astereoagnosia requires a high level of patient participation that would usually only occur in earlier disease phases. Thus, clinical-imaging correlations using MD alone is problematic, as it is not clear a priori whether something will correlate with increased or decreased MD; this limitation, however, can be overcome using a quantitative multi-parameter approach, such as our MRI Disease-Staging, that correlates with clinical outcomes only in one direction.

We are aware of only two other studies that have attempted to systematically correlate diffusion alterations and clinical deficits in PrD cohorts. Cohen *et. al. 2009*, working predominantly with E200K genetic CJD, which radiologically has much overlap with some sCJD subtypes, used visual assessment, rather than their quantitative MD ADC map data, for correlating DWI hyperintensity (allegedly decreased diffusion) with several neurological syndromes (Cohen et al., 2009). They found no correlation between cerebellar DWI hyperintensity and cerebellar syndrome (consistent with our MD findings), whereas DWI hyperintensity in the frontal lobe, precentral gyrus and basal ganglia correlated with executive function deficits, pyramidal and extrapyramidal syndrome, respectively. Although they also quantitatively measured MD from ADC maps, for reasons that are unclear to us, they only used DWI hyperintensity by visual assessment, and not this quantitative ADC data, for correlations with clinical symptoms. As visual assessment of DWI trace images is far less sensitive and more subject to artifact, and MD from DWI ADC maps is somewhat less sensitive than a quantification of MD derived from DTI (Alexander et al., 2007), in our analysis we explored the MD values (derived from DTI) of ROIs expected to be involved, looking for differences between subjects with or without certain symptoms. When we examined MD alone, however, we found that only subjects with left body astereognosis and/or agraphesthesia showed lower MD in the right postcentral gyrus, but no differences were detected in the ROIs expected to be involved between patients with or without pyramidal, extrapyramidal, cerebellar and visual symptoms (Table 4).

Several reasons can account for the discordance between our results and those of Cohen *et.al* 2009. Despite Cohen *et al.* having several cortical regions with DWI hyperintensity correlating with some neurological symptoms, with their quantitative approach (measuring MD from Apparent Diffusion Coefficient maps) did not find any cortical regions with decreased MD; this might suggest that some, or much, of the cortical DWI hyperintensity was artifact rather than true reduced diffusion. DWI images can be subject to artifact, particularly in frontal regions, from susceptibility effects in regions adjacent to the sinuses (Pierpaoli, 2010; Pierpaoli et al., 2001; Zerr et al., 2009). This might explain the difference between our findings, which correlat with true and quantified MD rather than DWI hyperintensity of unclear diffusion level. Lastly, another possible reason for different findings between our study and Cohen *et al.* is that although E200K has overlap with sCJD, clinicopathologically they are not quite equivalent (Brown et al., 1986, 1994; Brownell and Oppenheimer, 1965; Chapman et al., 1993; Cohen et al., 2011; Collins et al., 2006; Cooper et al., 2005; Kropp et al., 1999; Parchi et al., 1999; Takada et al., 2017; Tsuji et al., 2004).

The second study that correlated diffusion alterations with clinical presentation in a PrD cohort was by De Vita et al., 2013. Somewhat similarly to our study, they approached the clinical-imaging correlations with a multi-parametric quantitative MRI analysis, conducting a voxel based analysis of MD maps, which was, however, derived from DWI, not DTI (De Vita et al., 2013). Also, differently from us, their analysis was of only nine subjects, all with a six octapeptide repeat insertion mutation (6-OPRI)) that usually causes a Gerstmann-Sträussler-Scheinker form of gPrD that does not show restricted diffusion on MRI (Takada et al., 2017; Kim et al., 2018; Boxer et al., 2007). This is most likely because 6-OPRI cases radiologically might be more similar to other non-prion neurodegenerative disease which show increased MD with progression (Kantarci et al., 2010; Whitwell et al., 2010). Thus, not unexpectedly in this study, differently from ours and Cohen *et al.'s* findings, clinical deficits were associated only with increased MD values.

A second reason why our MRI Disease-Staging, combining both MD and Volume changes, works better for clinical-imaging correlation than MD changes alone is that in general MD increases at a later disease stage, around the time when atrophy occurs (Grau-Rivera et al., 2017; Iwasaki, 2017; Iwasaki et al., 2014). As MD in sCJD has a quaisi-J or U-shaped curve (Caverzasi et al., 2014a; Grau-Rivera et al., 2017), when MD is still normal, one cannot tell if it is in the early, downslope of MD (decreasing MD phase) or in the later, upslope (increasing MD phase). As within each subject at a single time point different brain regions might be in different stages of disease (Grau-Rivera et al., 2017), it suggests that the clinical history cannot give reliable suggestions on where different brain regions might be along the quasi J- or U-shaped curve of the longitudinal MD change. If significant brain atrophy were present by visual assessment, this could suggest that most brain regions are in advanced disease stages. Most sCJD subjects do not show gross atrophy by visual assessment of MRI. Assuming that atrophy is present but not detectable by visual assessment, adding quantification of Volume to the equation may help resolve this issue. If there is no atrophy, one is likely still early and in the decreasing phase and if atrophy is present, one likely is in the increasing MD phase. Thus, the combined MD-Volume assessment helps determine if areas with normal MD values are normal because 1. The areas are either not involved (MRI-Disease Stage 0) or 2. MD is "pseudo-normalized," as it is on the increasing phase of the quasi J- or U-shaped curve when Volume loss is present (MRI-Disease Stage 3). Next we discuss how Volume loss might affect MD changes in sCJD.

Regarding the histopathology underlying MD change over time, our current data support the possible influence of Volume loss on MD values. First, we found a negative correlation between Volume and MD z-score in all GM ROIs (Table 3), suggesting that when Volume is reduced, MD is increased. Second, our MRI-Disease Stage accounting for MD and Volume correlated with more clinical outcomes than either MD or Volume alone. Some of the earliest pathological changes in sCJD are PrP^{Sc} deposition and small vacuolation, followed by a phase of increasing gliosis, and in later stages increasing neuronal loss with disruption of cytoarchitecture (neuropil rarefaction) up to, in some cases, a state defined as status spongiosus (severe gliosis, neuronal loss, and rarefaction) (Iwasaki, 2017; Iwasaki et al., 2014; Masters and Richardson, 1978). A few studies have tried to correlate sCJD pathological changes with MD and Volume changes. Reduced MD associates best with earliest pathological changes, including PrP^{Sc} deposition (Geschwind et al., 2009; Haïk et al., 2002) and particularly microvacuolation (Geschwind et al., 2009; Manners et al., 2009). Neuronal loss, disruption of brain cytoarchitecture and severe reactive gliosis are likely to increase MD (Grau-Rivera et al., 2017; Haïk et al., 2008; Ukisu et al., 2005), as is seen also in other neurodegenerative diseases (Kantarci et al., 2010; Whitwell et al., 2010). Other possible key factors in the pseudo-normalization or even increase of the MD signal in sCJD might be the coalescence of vacuoles and expansion of the size of each vacuole, both of which can occur in later stages (Masters and Richardson, 1978). If vacuoles enlarge sufficiently, such as in status spongiosus, the diffusion of water might no longer be restricted (Gelal et al., 2002; Geschwind et al., 2009).

Although our study is cross-sectional, it suggests progressive increase in MD with the development and progression of atrophy as well as disability. This is supported by our finding that subjects with lower Barthel and subjects later in their disease course (larger Time-Ratio) both showed a greater proportion of more advanced MRI Disease-Stages than subjects with higher Barthel or subjects earlier in their disease course (lower Time-Ratio), respectively. A paper by Park et al. also supports increasing or at least pseudo-normalization of MD in later sCJD stages, when atrophy is present. They divided their cross-sectional 36 sCJD codon 129MM cases clinically into four disease-stage groups (1. vague symptomatic, 2. possible CJD criteria, 3. probably CJD criteria and 4. chronic vegetative state characterized by full dementia and akinetic mutism) and compared the pattern of involvement on DWI and ADC map by visual assessment among these stages (Park et al., 2016). DWI signal cortical hyperintensities increased from the first stage to the

third stage, but then became less hyperintense in the last clinical stage. Such a finding of decreased DWI hyperintensities in later clinical stages has been reported elsewhere as well (Eisenmenger et al., 2016; Hirose et al., 1998; Matoba et al., 2001; Oppenheim et al., 2004; Tribl et al., 2002; Ukisu et al., 2005). This finding is very consistent with our model suggesting increasing MD in later stages, particularly in the cortex. Park et al. also found that striatal DWI/ADC involvement in their MM cases occurred in later disease stages, which was consistent with our data showing lower MD MD in the striatum of more impaired patients (Fig. 2A).

A longitudinal DTI study might confirm our hypothesis of MD quasi J-shape changes over time, but given the rarity of the disease and its rapid course, acquiring serial MRIs in sCJD of sufficient quality for quantitative MD analysis has been difficult (Caverzasi et al., 2014a; Grau-Rivera et al., 2017). We are only aware of two cohort studies, both on a limited number of subjects, that have longitudinally assessed quantitative MD changes, and they showed conflicting results. Our prior study in seven subjects with serial scans found trends toward increasing MD in several regions (caudate, thalamus and many cortical regions), but decreasing MD in a few cortical regions (Caverzasi et al., 2014a). The second study with seven subjects imaged serially, however, found decreasing MD only in the left striatum, but no other changes (Eisenmenger et al., 2016). We believe there are some technical differences between Caverzasi et al. 2014a and Eisenmenger et al., 2016 that might explain the different findings. In the analysis of these conflicting results, however, it has to be noted also that an individual with sCJD can simultaneously have some regions with increased MD, some with decreased MD, and some with normal MD (Grau-Rivera et al., 2017). This is because in affected brain regions, initially there is a phase of decreased MD that if the disease progresses for long enough time, it is followed by a stage of increasing MD (Caverzasi et al., 2014a). The most common molecular sCJD subtypes (MV1 and MM1) show involvement of both cortical and subcortical GM, but this involvement does not necessarily occur synchronously. Our data in Fig. 2A show that that the course of MD changes within the subcortical GM (reduced MD) might, indeed, not be in the same phase on the quasi J-shape curve as cerebellar and cortical changes. As shown in Fig. 2A, subjects with lower Barthel (later in the disease) have lower MD than those with higher Barthel scores (earlier in the disease), suggesting that subcortical MD is lagging behind cortical and cerebellar MD on the quasi J-shape curve of MD change. Thus, a possible explanation for the finding of longitudinal decreasing MD within the basal ganglia in Eisenmenger et al., 2016 may be due to the different timing of involvement of the subcortical compared to the cortical GM in sCJD. This is further supported by a recent longitudinal quantitative MRI analysis of a single sCJD subject with seven MRI scans, including five DTI acquisitions, from 4th to 17th months from disease onset (Vitali et al., 2019). This paper showed a pattern of early cortical and later striatum involvement, suggesting cortical-subcortical spreading of the disease (which we find commonly in our clinical experience). A finding of further interest in Vitali et al., 2019 was that the early cortical involvement with restricted diffusion was associated with early cognitive impairtment, whereas the late striatal restricted diffusion was associated with late extrapyramidal motor impairment. In the context of a cortical-subcortical spreading, with involvement of subcortical gray matter typically occurring in later stages of the disease, it is conceivable that whereas within the cortex it is possible to detect the full spectrum along the quasi J-shaped curve of MD changes, within the basal ganglia and particularly in the striatum, which are on the earlier parts of the quasi J-shaped curve with reduced MD, one might not be able to detect pseudo-normalization or increased MD at the time of the subjects last MRI or prior to their death.

We will now address why our MRI Disease-Staging scale, combining MD and Volume changes, works better for clinical-imaging correlation than Volume changes alone. Volume loss by visual assessment is usually not noted in sCJD and other prion diseases, and when evident, it is usually only in late disease stages, and often in patients with long courses (Uchino et al., 1991; Finkenstaedt et al., 1996; De Vita et al., 2017). Therefore, atrophy might not be expected to correlate with focal clinical deficits in early stages, but in later stages could correlate with focal deficits and general function. Symptoms present at the onset are likely to be associated with the initial histopathological alterations of the disease (vacuolation and PrP^{Sc} deposition) more than neuronal loss, which develop in later stages. In a longitudinal VBM analysis of a subcohort of 21 subjects with prion disease (mostly with slowly progressive genetic forms and only 2 sCJD cases) whom had serial imaging with interscan intervals of >3 months, De Vita et al. found Volume loss in each of several brain regions correlated with functional decline (De Vita et al., 2017). In a different study, the same research group performed VBM on 23 cases of various forms of PrDs (mostly gPrD, unclear how many sCJD) who had detailed neurocognitive assessment. Using principal component analysis, they found a major axis of fronto-parietal dysfunction on cognitive testing that correlated with Volume loss in frontal and parietal gray matter (Caine et al., 2015). In our current study, similar to the previous literature, Volume loss in various ROIs correlated significantly with functional decline (e.g., Barthel and MMSE). We also found focal motor and pre-motor cortex Volume loss correlated with a contralateral pyramidal syndrome. The correlations between these clinical scores and Volume in most GM ROIs suggests that as disease progresses, functional decline is associated with atrophy. The lack of correlation between Time-Ratio and Volume is, however, probably due to the fact that not all subjects, particularly those with short disease duration, develop significant atrophy.

There are few other interesting aspects emerged from our analysis that need to be discussed. One issue is the lack of correlation between the amount of brain involved by either Volume loss or MD alterations (expressed as percent of VOIs or percent of brain volume with MRI disease-stage 1 to 4) and measures of disease severity such as Time-Ratio and Barthel. One might have expected the amount of brain volume involved to increase along with greater functional impairment (lower Barthel) as well as progression through later stages (higher Time-Ratio). One reasons for our finding might be that which specific VOIs, rather than the number of VOIs, involved are more relevant to clinical impairment. In our experience, this is perhaps best exemplified by our observation that many sCJD patients with extensive diffuse cortical restricted diffusivity by visual assessment are often surprisingly intact functionally and motorically, yet patients with limited cortical and but significant deep nuclei involvement can be very impaired.

For both Volume and MD, changes within cerebellar ROIs correlated strongly with MMSE and Barthel. Interestingly, in our analysis, there was however no relationship between presence of a cerebellar syndrome and quantitative metrics values (MD, Volume, MRI Disease-Stage). There are a few possible reasons for this. One is that the Freesurfer segmentation used for our analysis includes only two cerebellar hemispheric VOIs. The classic anatomical and functional subdivision of the cerebellum includes 3 lobes: inferior, superior and anterior lobe. Each one of these lobes is connected with specific cerebellar subcortical nuclei as well as with specific areas of brain and spinal cord. Each specific lobe is therefore associated with specific symptoms and syndromes (Tanabe et al., 2018). Furthermore, data suggests that the anterior cerebellum is more associated with motor control, whereas the posterior cerebellum is more related to cognitive and affective function (Stoodley and Schmahmann, 2010; Argyropoulos et al., 2020) The use of a hemispheric ROIs does not take in account the lobar subdivision and might therefore limit our ability to detect a relationship with the different cerebellar syndromes. Improved methodologies for parcellating the cerebellum on MRI studies hopefully should facilitate these types of analyses and we plan to implement these when they become more widely available. Another possible reason for the lack of correlation of MRI findings with the presence or absence of a cerebellar syndrome is that the cerebellar deficits might be arising outside of the cerebellum, from regions connected with the cerebellum. Changes within hemispheric cerebellar ROIs did correlate, however, with clinical scores such as the Barthel and

MMSE, which more grossly assess the functional and cognitive status of the subjects. This suggests that the cerebellum might have an important role in the development of these deficits, which as noted needs to be further assessed with a more specific segmentation of cerebellar structures possibly including cerebellar lobes, as well as subcortical GM nuclei.

MD was the only MRI quantitative metric that correlated with neuropsychiatric symptoms. Specifically, the Total NPI correlated inversely with subcortical MD (higher the NPI, the lower the MD), whereas aberrant motor behavior correlated inversely with anterior cingulate MD. As suggested by our experience as well as prior literature (Thompson et al., 2015), we think this might be related to the psychiatric symptoms being more evident in earlier compared to later sCJD phases. This might be because, with disease progression to more advanced phases, the psychiatric symptoms actually decline or become simply not as noticeable due to other features potentially overshadowing them (severe dementia, aphasia, akinetic mutism, etc…).

Our study has several limitations. Our cohort is small for a typical dementia study but large for a quantitative imaging study in prion disease and has the advantages being clinically very thoroughly characterized with quantitative assessment of diffusion data homogeneously acquired at a single site. Furthermore, our cohort has been assessed for complete codon 129 polymorphism data, which alone has been shown to have a significant effect on the clinical course even without prion typing information (Mead et al., 2016). Nonetheless we are aware that our method should be ideally validated with a larger representation of sCJD subtypes in order to confirm its robustness, particularly when considering the high phenotypic variability of this disease. Our cohort shows, indeed, a different proportion of the three codon 129 subtypes compared to other large multinational cohorts, specifically a lower number of MM molecular subtypes, which one study has shown to be associated with short disease duration (Mead et al., 2016). This is probably because the MM1 subtype, which is the most common in large autopsy studies, typically progresses very rapidly with severe dementia, ataxia and myoclonus, making it difficult to obtain sufficient quality research MRIs for such analyses. A large multicenter approach may be useful in the future in order to obtain a better representative sample of sCJD subtypes. Although this study did not include histopathological correlations, our use of very conservative thresholds to score a region or Volume (-2 SD and $+2$ SD for MD and -2 SD for Volume versus controls) in an sCJD case as being involved supports the strength of our radiological findings. Future studies in a cohort with short intervals between MRI and death, although difficult to obtain, might allow inclusion of histopathological correlations with MRI findings. In the current study, for Volume computation we used a VBM approach with the data of each subject being transferred within the MNI space. We realize this is different from the surfaced-based analysis (SBA) with Freesurfer used in the previous study of our group (Caverzasi et al 2014a) in which we worked on each single subject space and used data on cortical thickness computed trough Freesurfer. The only reason why in the present study we decided to use a VBM approach, rather than replicate the SBA approach used in our previous work is that the standard pipeline now in use within our center uses VBM rather than Freesurfer. It is important to note that VBM Volume computation and Freesurfer cortical thickness assessment are both comparable methods to detect atrophy. We are not aware of any convincing data showing significant superiority in atrophy detection of one method over the other.

Longitudinal studies in larger sCJD cohorts are needed to further demonstrate the nature of the course of MD changes over-time as well as to better time the onset and progression of atrophy. These studies could further assess the validity of our MRI Disease-Staging.

5. Conclusion

This study showed that the clinical-radiological correlation in sCJD can be improved by the use of an MRI Disease-Staging combining MD abnormalties and Volume loss. Due to the non-linear course of MD overtime, its role alone as a non-invasive biomarker is problematic. An MRI Disease-Staging based on reduced MD and normal Volume early in the disease, followed by phases of normal/increased MD and reduced Volume might be a better approach for tracking sCJD progression in clinical studies and trials.

Author contributions

Simone Sacco: conceptualization and design, analysis and interpretation of data, drafting the article and revising it critically.

Matteo Paoletti: conceptualization and design, acquisition of data, methodology, critical revision of the article.

Adam Staffaroni: analysis and interpretation of data, methodology, critical revision of the article

Huicong Kang: analysis and interpretation of data, critical revision of the article

Julio Rojas: analysis and interpretation of data, critical revision of the article.

Gabe Marx: acquisition of data, analysis and interpretation of data.

Sheng-yanhg Goh: acquisition of data, analysis and interpretation of data.

Maria Luisa Mandelli: methodology, critical revision of the article

Isabel E. Allen: methodology, critical revision of the article.

Joel H. Kramer: supervision, critical revision of the article.

Stefano Bastianello: supervision, critical revision of the article.

Roland G. Henry: supervision, critical revision of the article

Howie. J. Rosen: supervision, critical revision of the article

Eduardo Caverzasi: conceptualization and design, analysis and interpretation of data, critical revision of the article.

Michael D. Geschwind: conceptualization and design, supervision, acquisition of data, analysis and interpretation of data, critical revision of the article

Disclosures

SS, EC, MP, AS, HK, JR, GM, SYH, IEA, JHK, SB, RGH, HJR have no conflict of interest related to this paper. MDG has no conflicts directly related to this paper; he currently receives research support on prion disease from the NIH/NIA (R56 AG055619) and the Michael J. Homer Family Fund. He has consulted for Adept Field Consulting (Backay consulting), Advanced Medical Inc., Anderson Boutwell Traylor, Ascel Health LLC, Best Doctors Inc., Blade Therapeutics, Biohaven Pharmaceuticals, Bioscience Pharma Partners, LLC (BPP), ClearView HealthCare Partners, Grand Rounds Inc./Second Opinion Inc., Gerson Lehrman Group (GLG) Inc., Guidepoint Global LLC, Market Plus, InThought Consulting, LifeSci Capital LLC, Maupin Cox Legoy, MEDACorp, Quest Diagnostics, 3MCommunications (Microvention Terumo), Smith & Hennessey LLC, and Trinity Partners LLC. He has received speaking honoraria for various medical center lectures and from Oakstone Publishing. He has received past research support from Alliance Biosecure, CurePSP, the Tau Consortium, Quest Diagnostics, and NIH. Dr. Geschwind serves on the board of directors for San Francisco Bay Area Physicians for Social Responsibility and on the editorial board of Dementia & Neuropsychologia.

Acknowledgements

The authors would like to thank our patients and their families for participating in our research; referring physicians; the U.S. National Prion Disease Pathology Surveillance Center (NPDPSC) for assistance with *PRNP* analyses, prion typing and pathological analyses; Stephen J. DeArmond, MD, PhD and Henry Sanchez, MD for pathological assistance; the U.S. CJD Foundation (for supporting our patients and families). This work was supported by National Institutes of Health, National Institute of Aging (NIH/NIA) R01 AG031189, NIH/NCRR UL1

RR024131, NIH/NIA AG031220, P50AG023501, NIH/NIAAG021601, and The Michael J. Homer Family Foundation. S.S., M.P., and E.C. were supported by University of Pavia, Italy.

Appendix A. Supplementary data

Supplementary data to this article can be found online at https://doi.org/10.1016/j.nicl.2020.102523.

References

Alexander, A.L., Lee, J.E., Lazar, M., Field, A.S., 2007. Diffusion tensor imaging of the brain. Neurotherapeutics 4 (3), 316–329. https://doi.org/10.1016/j.nurt.2007.05.011.

Alner, K., Hyare, H., Mead, S., Rudge, P., Wroe, S., Rohrer, J.D., Ridgeway, G., Ourselin, S., Clarkson, M., Hunt, H., et al., 2011. Distinct neuropsychological profiles correspond to distribution of cortical thinning in inherited prion disease caused by insertional mutation. J. Neurol. Neurosurg. Psychiatr.

Appleby, B.S., Appleby, K.K., Crain, B.J., Onyike, C.U., Wallin, M.T., Rabins, P.V., 2009. Characteristics of established and proposed sporadic Creutzfeldt-Jakob disease variants. Arch. Neurol. 66, 208–215.

Argyropoulos, G.P.D., van Dun, K., Adamaszek, M., Leggio, M., Manto, M., Masciullo, M., Molinari, M., Stoodley, C.J., Van Overwalle, F., Ivry, R.B., Schmahmann, J.D., 2020. The cerebellar cognitive affective/Schmahmann syndrome: A task force paper. Cerebellum 19 (1), 102–125. https://doi.org/10.1007/s12311-019-01068-8.

Ashburner, J., Friston, K.J., 2005. Unified segmentation. NeuroImage 26 (3), 839–851. https://doi.org/10.1016/j.neuroimage.2005.02.018.

Ashburner, J., Friston, K.J., 2011. Diffeomorphic registration using geodesic shooting and Gauss–Newton optimisation. NeuroImage 55 (3), 954–967. https://doi.org/10.1016/j.neuroimage.2010.12.049.

Baldo, J.V., Arévalo, A., Patterson, J.P., Dronkers, N.F., 2013. Grey and white matter correlates of picture naming: Evidence from a voxel-based lesion analysis of the Boston Naming Test. Cortex 49 (3), 658–667. https://doi.org/10.1016/j.cortex.2012.03.001.

Baldo, Juliana.V., Schwartz, Sophie, Wilkins, David, Dronkers, Nina.F., 2006. Role of frontal versus temporal cortex in verbal fluency as revealed by voxel-based lesion symptom mapping. J. Inter. Neuropsych. Soc. 12 (06) https://doi.org/10.1017/S1355617706061078.

Benjamini, Y., Hochberg, Y., 1995. Controlling the false discovery rate: A practical and powerful approach to multiple testing. J. R. Statistical Soc. Ser. B Methodol. 57 (1), 289–300. https://doi.org/10.1111/j.2517-6161.1995.tb02031.x.

Birn, R.M., Kenworthy, L., Case, L., Caravella, R., Jones, T.B., Bandettini, P.A., Martin, A., 2010. Neural systems supporting lexical search guided by letter and semantic category cues: A self-paced overt response fMRI study of verbal fluency. NeuroImage 49 (1), 1099–1107. https://doi.org/10.1016/j.neuroimage.2009.07.036.

Brown, P., Cathala, F., Castaigne, P., Gajdusek, D.C., 1986. Creutzfeldt-Jakob disease: Clinical analysis of a consecutive series of 230 neuropathologically verified cases. Ann. Neurol. 20 (5), 597–602. https://doi.org/10.1002/ana.410200507.

Brown, P., Gibbs, C.J., Rodgers-Johnson, P., Asher, D.M., Sulima, M.P., Bacote, A., Goldfarb, L.G., Gajdusek, D.C., 1994. Human spongiform encephalopathy: The national institutes of health series of 300 cases of experimentally transmitted disease. Ann. Neurol. 35 (5), 513–529. https://doi.org/10.1002/ana.410350504.

Brownell, B., Oppenheimer, D.R., 1965. An ataxic form of subacute presenile polioencephalopathy (Creutzfeldt-Jakob disease). J. Neurol. Neurosurg. Psychiatr. 28 (4), 350–361. https://doi.org/10.1136/jnnp.28.4.350.

Boxer, A.L., Rabinovici, G.D., Kepe, V., Goldman, J., Furst, A.J., Huang, S.C., Baker, S.L., O'neil, J.P., Chui, H., Geschwind, M.D., Small, G.W., Barrio, J.R., Jagust, W., Miller, B.L., 2007. Amyloid imaging in distinguishing atypical prion disease from Alzheimer disease. Neurology. 69 (3), 283–290. https://doi.org/10.1212/01.wnl.0000265815.38958.b6. PMID: 17636066.

Caine, D., Tinelli, R.J., Hyare, H., De Vita, E., Lowe, J., Lukic, A., Thompson, A., Porter, M.C., Cipolotti, L., Rudge, P., Collinge, J., Mead, S., 2015. The cognitive profile of prion disease: a prospective clinical and imaging study. Ann Clin Transl Neurol. 2 (5), 548–558. https://doi.org/10.1002/acn3.195. Epub 2015 Apr 7 PMID: 26000326.

Caverzasi, E., Henry, R.G., Vitali, P., Lobach, I.V., Kornak, J., Bastianello, S., DeArmond, S.J., Miller, B.L., Rosen, H.J., Mandelli, M.L., Geschwind, M.D., 2014a. Application of quantitative DTI metrics in sporadic CJD. NeuroImage Clin. 4, 426–435. https://doi.org/10.1016/j.nicl.2014.01.011.

Caverzasi, E., Mandelli, M.L., DeArmond, S.J., Hess, C.P., Vitali, P., Papinutto, N., Oehler, A., Miller, B.L., Lobach, I.V., Bastianello, S., et al., 2014b. White matter involvement in sporadic Creutzfeldt-Jakob disease. Brain 137, 3339–3354.

Chapman, J., Brown, P., Goldfarb, L.G., Arlazoroff, A., Gajdusek, D.C., Korczyn, A.D., 1993. Clinical heterogeneity and unusual presentations of Creutzfeldt-Jakob disease in Jewish patients with the PRNP codon 200 mutation. J. Neurol. Neurosurg. Psychiatr. 56 (10), 1109–1112. https://doi.org/10.1136/jnnp.56.10.1109.

Chow, T.W., Cummings, J.L., 2007.). Chapter 3. Frontal-subcortical circuits, second edition. The Guilford Press, New York, pp. 3–26.

Cohen, O.S., Chapman, J., Lee, H., Nitsan, Z., Appel, S., Hoffman, C., Rosenmann, H., Korczyn, A.D., Prohovnik, I., 2011. Pruritus in familial Creutzfeldt–Jakob disease: a common symptom associated with central nervous system pathology. J. Neurol. 258 (1), 89–95. https://doi.org/10.1007/s00415-010-5694-1.

Cohen, O.S., Hoffmann, C., Lee, H., Chapman, J., Fulbright, R.K., Prohovnik, I., 2009. MRI detection of the cerebellar syndrome in Creutzfeldt–Jakob Disease. Cerebellum 8 (3), 373–381. https://doi.org/10.1007/s12311-009-0106-8.

Collins, S.J., Sanchez-Juan, P., Masters, C.L., Klug, G.M., van Duijn, C., Poleggi, A., Pocchiari, M., Almonti, S., Cuadrado-Corrales, N., de Pedro-Cuesta, J., et al., 2006. Determinants of diagnostic investigation sensitivities across the clinical spectrum of sporadic Creutzfeldt-Jakob disease. Brain 129, 2278–2287.

Cooper, S.A., Murray, K.L., Heath, C.A., Will, R.G., Knight, R.S.G., 2005. Isolated visual symptoms at onset in sporadic Creutzfeldt-Jakob disease: the clinical phenotype of the "Heidenhain variant". Br. J. Ophthalmol. 89, 1341–1342.

Cummings, Jeffrey.L., 1995. Anatomic and behavioral aspects of frontal-subcortical circuits. Ann. NY Acad. Sci. 769, 1–13. https://doi.org/10.1111/j.1749-6632.1995.tb38127.x.

Cummings, J.L., 1997. The Neuropsychiatric Inventory: Assessing psychopathology in dementia patients. Neurology 48, S10–S16. https://doi.org/10.1212/WNL.48.5_Suppl_6.10S.

De Vita, E., Ridgway, G.R., Scahill, R.I., Caine, D., Rudge, P., Yousry, T.A., Mead, S., Collinge, J., Jäger, H.R., Thornton, J.S., Hyare, H., 2013. Multiparameter MR imaging in the 6-OPRI variant OF inherited Prion Disease. AJNR Am. J. Neuroradiol. 34 (9), 1723–1730. https://doi.org/10.3174/ajnr.A3504.

De Vita, E., Ridgway, G.R., White, M.J., Porter, M.-C., Caine, D., Rudge, P., Collinge, J., Yousry, T.A., Jager, H.R., Mead, S., Thornton, J.S., Hyare, H., 2017. Neuroanatomical correlates of prion disease progression - a 3T longitudinal voxel-based morphometry study. NeuroImage Clin. 13, 89–96. https://doi.org/10.1016/j.nicl.2016.10.021.

Desikan, R.S., Ségonne, F., Fischl, B., Quinn, B.T., Dickerson, B.C., Blacker, D., Buckner, R.L., Dale, A.M., Maguire, R.P., Hyman, B.T., Albert, M.S., Killiany, R.J., 2006. An automated labeling system for subdividing the human cerebral cortex on MRI scans into gyral based regions of interest. NeuroImage 31 (3), 968–980. https://doi.org/10.1016/j.neuroimage.2006.01.021.

Eisenmenger, L., Porter, M.-C., Carswell, C.J., Thompson, A., Mead, S., Rudge, P., Collinge, J., Brandner, S., Jäger, H.R., Hyare, H., 2016. Evolution of Diffusion-Weighted Magnetic Resonance Imaging Signal Abnormality in Sporadic Creutzfeldt-Jakob Disease, With Histopathological Correlation. JAMA Neurol. 73 (1), 76. https://doi.org/10.1001/jamaneurol.2015.3159.

Fernandez-Torre, J.L., Freeman, W.D., Shuster, E., Brazis, P., Dickson, D., Lapergue, B., Navarro, V., 2011. Sporadic Creutzfeldt-Jakob disease mimicking nonconvulsive status epilepticus. Neurology 76 (12), 1111–1112. https://doi.org/10.1212/WNL.0b013e31820a9535.

Finkenstaedt, M., Szudra, A., Zerr, I., Poser, S., Hise, J.H., Stoebner, J.M., Weber, T., 1996. MR imaging of Creutzfeldt-Jakob disease. Radiology 199 (3), 793–798. https://doi.org/10.1148/radiology.199.3.8638007.

Fischl, B., Salat, D.H., Busa, E., Albert, M., Dieterich, M., Haselgrove, C., van der Kouwe, A., Killiany, R., Kennedy, D., Klaveness, S., Montillo, A., Makris, N., Rosen, B., Dale, A.M., 2002. Whole brain segmentation. Neuron 33 (3), 341–355. https://doi.org/10.1016/S0896-6273(02)00569-X.

Folstein, M.F., Folstein, S.E., McHugh, P.R., 1975. "Mini-mental state". J. Psychiatr. Res. 12 (3), 189–198. https://doi.org/10.1016/0022-3956(75)90026-6.

Galvez, S., Cartier, L., 1984. Computed tomography findings in 15 cases of Creutzfeldt-Jakob disease with histological verification. J. Neurol. Neurosurg. Psychiatr. 47 (11), 1244–1246. https://doi.org/10.1136/jnnp.47.11.1244.

Gelal, F., Callı, C., Apaydın, M., Erdem, G., 2002. van der Knaap's leukoencephalopathy: Report of five new cases with emphasis on diffusion-weighted MRI findings. Neuroradiology 44 (7), 625–630. https://doi.org/10.1007/s00234-002-0748-4.

Geschwind, M.D., Josephs, K.A., Parisi, J.E., Keegan, B.M., 2007. A 54-year-old man with slowness of movement and confusion. Neurology 69 (19), 1881–1887. https://doi.org/10.1212/01.wnl.0000290370.14036.69.

Geschwind, M.D., Kuo, A.L., Wong, K.S., Haman, A., Devereux, G., Raudabaugh, B.J., Johnson, D.Y., Torres-Chae, C.C., Finley, R., Garcia, P., Thai, J.N., Cheng, H.Q., Neuhaus, J.M., Forner, S.A., Duncan, J.L., Possin, K.L., DeArmond, S.J., Prusiner, S. B., Miller, B.L., 2013. Quinacrine treatment trial for sporadic Creutzfeldt-Jakob disease. Neurology 81 (23), 2015–2023. https://doi.org/10.1212/WNL.0b013e3182a9f3b4.

Geschwind, M.D., Potter, C.A., Sattavat, M., Garcia, P.A., Rosen, H.J., Miller, B.L., DeArmond, S.J., 2009. Correlating DWI MRI with pathologic and other features of Jakob-Creutzfeldt Disease: Alzheimer Dis. Assoc. Disord. 23 (1), 82–87. https://doi.org/10.1097/WAD.0b013e31818323ef.

Glickman, M.E., Rao, S.R., Schultz, M.R., 2014. False discovery rate control is a recommended alternative to Bonferroni-type adjustments in health studies. J. Clin. Epidemiol. 67, 850–857.

Grau-Rivera, O., Calvo, A., Bargalló, N., Monté, G.C., Nos, C., Lladó, A., Molinuevo, J.L., Gelpi, E., Sánchez-Valle, R., Zerr, I., 2017. Quantitative magnetic resonance abnormalities in Creutzfeldt-Jakob disease and fatal insomnia. JAD 55 (1), 431–443. https://doi.org/10.3233/JAD-160750.

Greve, D.N., Fischl, B., 2009. Accurate and robust brain image alignment using boundary-based registration. NeuroImage 48 (1), 63–72. https://doi.org/10.1016/j.neuroimage.2009.06.060.

Haïk, S., Dormont, D., Faucheux, B.A., Marsault, C., Hauw, J.-J., 2002. Prion protein deposits match magnetic resonance imaging signal abnormalities in Creutzfeldt-Jakob disease. Ann. Neurol. 51 (6), 797–799. https://doi.org/10.1002/ana.10195.

Haïk, S., Galanaud, D., Linguraru, M.G., Peoc'h, K., Privat, N., Faucheux, B.A., Ayache, N., Hauw, J.-J., Dormont, D., Brandel, J.-P., 2008. In Vivo Detection of Thalamic Gliosis: A pathoradiologic demonstration in familial fatal insomnia. Arch. Neurol. 65 (4), 545. https://doi.org/10.1001/archneur.65.4.545.

Hirose, Y., Mokuno, K., Abe, Y., Sobue, G., Matsukawa, N., 1998. A case of clinically diagnosed Creutzfeldt-Jakob disease with serial MRI diffusion weighted images. Rinsho Shinkeigaku 38, 779–782.
Iwasaki, Y., 2017. Creutzfeldt-Jakob disease: Creutzfeldt-Jakob disease. Neuropathology 37 (2), 174–188. https://doi.org/10.1111/neup.12355.
Iwasaki, Y., Tatsumi, S., Mimuro, M., Kitamoto, T., Hashizume, Y., Yoshida, M., 2014. Relation between clinical findings and progression of cerebral cortical pathology in MM1-type sporadic Creutzfeldt–Jakob disease: Proposed staging of cerebral cortical pathology. J. Neurol. Sci. 341 (1-2), 97–104. https://doi.org/10.1016/j.jns.2014.04.011.
Kantarci, K., Avula, R., Senjem, M.L., Samikoglu, A.R., Zhang, B., Weigand, S.D., Przybelski, S.A., Edmonson, H.A., Vemuri, P., Knopman, D.S., Ferman, T.J., Boeve, B.F., Petersen, R.C., Jack, C.R., 2010. Dementia with Lewy bodies and Alzheimer disease: Neurodegenerative patterns characterized by DTI. Neurology 74 (22), 1814–1821. https://doi.org/10.1212/WNL.0b013e3181e0f7cf.
Kim, M.O., Takada, L.T., Wong, K., Forner, S.A., Geschwind, M.D., 2018. Genetic PrP Prion Diseases. Cold Spring Harb Perspect Biol. 10 (5), a033134 https://doi.org/10.1101/cshperspect.a033134. PMID: 28778873.
Kramer, J.H., Jurik, J., Sha, S.J., Rankin, K.P., Rosen, H.J., Johnson, J.K., Miller, B.L., 2003. Distinctive neuropsychological patterns in frontotemporal dementia, semantic dementia, and Alzheimer Disease: Cognit. Behav. Neurol. 16 (4), 211–218. https://doi.org/10.1097/00146965-200312000-00002.
Kretzschmar, H.A., Ironside, J.W., DeArmond, S.J., Tateishi, J., 1996. Diagnostic criteria for sporadic Creutzfeldt-Jakob disease. Arch. Neurol. 53 (9), 913–920. https://doi.org/10.1001/archneur.1996.00550090125018.
Kropp, S., Schulz-Schaeffer, W.J., Finkenstaedt, M., Riedemann, C., Windl, O., Steinhoff, B.J., Zerr, I., Kretzschmar, H.A., Poser, S., 1999. The Heidenhain Variant of Creutzfeldt-Jakob Disease. Arch. Neurol. 56 (1), 55. https://doi.org/10.1001/archneur.56.1.55.
Manners, D.N., Parchi, P., Tonon, C., Capellari, S., Strammiello, R., Testa, C., Tani, G., Malucelli, E., Spagnolo, C., Cortelli, P., Montagna, P., Lodi, R., Barbiroli, B., 2009. Pathologic correlates of diffusion MRI changes in Creutzfeldt-Jakob disease. Neurology 72 (16), 1425–1431. https://doi.org/10.1212/WNL.0b013e3181a18846.
Masters, C.L., Richardson Jr., E.P., 1978. Subacute spongiform encephalopathy (Creutzfeldt-Jakob disease): The nature and progression of spongiform change. Brain 101 (2), 333–344. https://doi.org/10.1093/brain/101.2.333.
Matoba, M., Tonami, H., Miyaji, H., Yokota, H., Yamamoto, I., 2001. Creutzfeldt-Jakob disease: Serial changes on diffusion-weighted MRI: J. Comput. Assis. Tomogr. 25 (2), 274–277. https://doi.org/10.1097/00004728-200103000-00022.
Mazziotta, J.C., Toga, A.W., Evans, A., Fox, P., Lancaster, J., 1995. A probabilistic atlas of the human brain: theory and rationale for its development. NeuroImage 2 (2), 89–101. https://doi.org/10.1006/nimg.1995.1012.
Mead, S., Burnell, M., Lowe, J., Thompson, A., Lukic, A., Porter, M.-C., Carswell, C., Kaski, D., Kenny, J., Mok, T.H., Bjurstrom, N., Franko, E., Gorham, M., Druyeh, R., Wadsworth, J.D.F., Jaunmuktane, Z., Brandner, S., Hyare, H., Rudge, P., Walker, A. S., Collinge, J., 2016. Clinical trial simulations based on genetic stratification and the natural history of a functional outcome measure in Creutzfeldt-Jakob Disease. JAMA Neurol. 73 (4), 447. https://doi.org/10.1001/jamaneurol.2015.4885.
Mesulam, M.M., 2016. Primary Progressive Aphasia and the Left Hemisphere Language Network. Dement Neurocogn Disord. 15 (4), 93–102. https://doi.org/10.12779/dnd.2016.15.4.93. Epub 2016 Dec 31 PMID: 30906349.
Mesulam, M.M., 2000. Principles of Behavioral and Cognitive Neurology. Oxford University Press, New York.
Oppenheim, C., Zuber, M., Galanaud, D., Detilleux, M., Bolgert, F., Mas, J.L., Chiras, J., Meder, J.F., 2004. Spectroscopy and serial diffusion MR findings in hGH-Creutzfeldt-Jakob disease. J. Neurol. Neurosurg. Psychiatr. 75, 1066–1069.
Parchi, P., Giese, A., Capellari, S., Brown, P., Schulz-Schaeffer, W., Windl, O., Zerr, I., Budka, H., Kopp, N., Piccardo, P., Poser, S., Rojiani, A., Streichemberger, N., Julien, J., Vital, C., Ghetti, B., Gambetti, P., Kretzschmar, H., 1999. Classification of sporadic Creutzfeldt-Jakob disease based on molecular and phenotypic analysis of 300 subjects. Ann. Neurol. 46 (2), 224–233. https://doi.org/10.1002/1531-8249(199908)46:2<224::AID-ANA12>3.0.CO;2-W.
Park, S.Y., Wang, M.J., Jang, J.W., Park, Y.H., Lim, J.S., Youn, Y.C., Kim, J., Kim, S., 2016. The clinical stages of sporadic Creutzfeldt-Jakob disease with Met/Met Genotype in Korean patients. In: Eur. Neurol., 75, pp. 213–222.
Pierpaoli, C., 2010. Ch. 18 Artifacts in Diffusion MRI. Oxford University Press, Oxford; New York, p. xvi, 767 p.
Pierpaoli, C., Barnett, A., Pajevic, S., Chen, R., Penix, LaRoy, Virta, A., Basser, P., 2001. Water diffusion changes in wallerian degeneration and their dependence on white matter architecture. NeuroImage 13 (6), 1174–1185. https://doi.org/10.1006/nimg.2001.0765.
Prusiner, S.B., 1998. Prions. Proc. Natl. Acad. Sci. U.S.A. 95, 13363–13383.
Rabinovici, G.D., Wang, P.N., Levin, J., Cook, L., Pravdin, M., Davis, J., DeArmond, S.J., Barbaro, N.M., Martindale, J., Miller, B.L., Geschwind, M.D., 2006. First symptom in sporadic Creutzfeldt-Jakob disease. Neurology 66 (2), 286–287. https://doi.org/10.1212/01.wnl.0000196440.00297.67.
Rosen, H.J., Allison, S.C., Schauer, G.F., Gorno-Tempini, M.L., Weiner, M.W., Miller, B.L., 2005. Neuroanatomical correlates of behavioural disorders in dementia. Brain 128, 2612–2625.
Shah, S., Vanclay, F., Cooper, B., 1989. Improving the sensitivity of the Barthel Index for stroke rehabilitation. J. Clin. Epidemiol. 42 (8), 703–709. https://doi.org/10.1016/0895-4356(89)90065-6.
Shiga, Y., Miyazawa, K., Sato, S., Fukushima, R., Shibuya, S., Sato, Y., Konno, H., Doh-ura, K., Mugikura, S., Tamura, H., Higano, S., Takahashi, S., Itoyama, Y., 2004. Diffusion-weighted MRI abnormalities as an early diagnostic marker for Creutzfeldt-Jakob disease. Neurology 63 (3), 443–449. https://doi.org/10.1212/01.WNL.0000134555.59460.5D.
Staffaroni, A.M., Brown, J.A., Casaletto, K.B., Elahi, F.M., Deng, J., Neuhaus, J., Cobigo, Y., Mumford, P.S., Walters, S., Saloner, R., Karydas, A., Coppola, G., Rosen, H.J., Miller, B.L., Seeley, W.W., Kramer, J.H., 2018a. The Longitudinal trajectory of default mode network connectivity in healthy older adults varies as a function of age and is associated with changes in episodic memory and processing speed. J. Neurosci. 38 (11), 2809–2817. https://doi.org/10.1523/JNEUROSCI.3067-17.2018.
Staffaroni, A.M., Stephens, M.L., Kramer, J.H., 2018b. Bedside frontal lobe testing. In: Miller, B.L., Cummings, J.L. (Eds.), The Human Frontal Lobes: Functions and Disorders. The Guilford Press, pp. 124–136.
Stoodley, C.J., Schmahmann, J.D., 2010. Evidence for topographic organization in the cerebellum of motor control versus cognitive and affective processing. Cortex 46 (7), 831–844. https://doi.org/10.1016/j.cortex.2009.11.008.
Takada, L.T., Kim, M.O., Cleveland, R.W., Wong, K., Forner, S.A., Gala, I.I., Fong, J.C., Geschwind, M.D., 2017. Genetic prion disease: Experience of a rapidly progressive dementia center in the United States and a review of the literature. Am. J. Med. Genet. B Neuropsychiatr. Genet. 174, 36–69.
Tanabe, H.C., Kubo, D., Hasegawa, K., Kochiyama, T., Kondo, O., 2018. In: Digital Endocasts. Springer, Tokyo, pp. 275–289. https://doi.org/10.1007/978-4-431-56582-6_18.
Thompson, A., MacKay, A., Rudge, P., Lukic, A., Porter, M.C., Lowe, J., Collinge, J., Mead, S., 2014 Mar. Behavioral and psychiatric symptoms in prion disease. Am J Psychiatry. 171 (3), 265–274. https://doi.org/10.1176/appi.ajp.2013.12111460. PMID: 24585329.
Tribl, G., Strasser, G., Zeitlhofer, J., Asenbaum, S., Jarius, C., Wessely, P., Prayer, D., 2002. Sequential MRI in a case of Creutzfeldt-Jakob disease. Neuroradiology 44 (3), 223–226. https://doi.org/10.1007/s002340100695.
Tsuji, Y., Kanamori, H., Murakami, G., Yokode, M., Mezaki, T., Doh-ura, K., Taniguchi, K., Matsubayashi, K., Fukuyama, H., Kita, T., Tanaka, M., 2004. Heidenhain variant of Creutzfeldt-Jakob disease: diffusion-weighted MRI and PET characteristics. J. Neuroimaging 14, 63–66.
Uchino, A., Yoshinaga, M., Shiokawa, O., Hata, H., Ohno, M., 1991. Serial MR imaging in Creutzfeldt-Jakob disease. Neuroradiology 33 (4), 364–367. https://doi.org/10.1007/BF00587828.
Ukisu, R., Kushihashi, T., Kitanosono, T., Fujisawa, H., Takenaka, H., Ohgiya, Y., Gokan, T., Munechika, H., 2005. Serial diffusion-weighted MRI of Creutzfeldt-Jakob disease. Am. J. Roentgenol. 184 (2), 560–566. https://doi.org/10.2214/ajr.184.2.01840560.
Vitali, P., Maccagnano, E., Caverzasi, E., Henry, R.G., Haman, A., Torres-Chae, C., Johnson, D.Y., Miller, B.L., Geschwind, M.D., 2011. Diffusion-weighted MRI hyperintensity patterns differentiate CJD from other rapid dementias. Neurology 76 (20), 1711–1719. https://doi.org/10.1212/WNL.0b013e31821a4439.
Vitali, P., Palesi, F., Cotta Ramusino, M., Pan, M., Costa, A., Gandini Wheeler-Kingshott, C., Ceroni, M., Micieli, G., Anzalone, N., Giaccone, G., Tagliavini, F., Geschwind, M., 2019. Early cortical and late striatal diffusion restriction on 3T MRI in a long-lived sporadic creutzfeldt–jakob disease case. J. Magn. Reson. Imaging 50 (5), 1659–1662. https://doi.org/10.1002/jmri.26711.
Whitwell, J.L., Avula, R., Senjem, M.L., Kantarci, K., Weigand, S.D., Samikoglu, A., Edmonson, H.A., Vemuri, P., Knopman, D.S., Boeve, B.F., Petersen, R.C., Josephs, K. A., Jack, C.R., 2010. Gray and white matter water diffusion in the syndromic variants of frontotemporal dementia. Neurology 74 (16), 1279–1287. https://doi.org/10.1212/WNL.0b013e3181d9edde.
Zerr, I., Kallenberg, K., Summers, D.M., Romero, C., Taratuto, A., Heinemann, U., Breithaupt, M., Varges, D., Meissner, B., Ladogana, A., Schuur, M., Haik, S., Collins, S.J., Jansen, G.H., Stokin, G.B., Pimentel, J., Hewer, E., Collie, D., Smith, P., Roberts, H., Brandel, J.P., van Duijn, C., Pocchiari, M., Begue, C., Cras, P., Will, R.G., Sanchez-Juan, P., 2009. Updated clinical diagnostic criteria for sporadic Creutzfeldt-Jakob disease. Brain 132 (10), 2659–2668. https://doi.org/10.1093/brain/awp191.